DOCUMENT

DE TRAVAIL

N° 589

**UK TERM STRUCTURE DECOMPOSITIONS
AT THE ZERO LOWER BOUND**

Andrea Carriero, Sarah Mouabbi and Elisabetta Vangelista

April 2016

BANQUE DE FRANCE

EUROSYSTÈME

DIRECTION GÉNÉRALE DES ÉTUDES ET DES RELATIONS INTERNATIONALES

DIRECTION GÉNÉRALE DES ÉTUDES ET DES RELATIONS INTERNATIONALES

**UK TERM STRUCTURE DECOMPOSITIONS
AT THE ZERO LOWER BOUND**

Andrea Carriero, Sarah Mouabbi and Elisabetta Vangelista

April 2016

UK Term Structure Decompositions at the Zero Lower Bound

Andrea Carriero

Queen Mary, University of London

Sarah Mouabbi

Banque de France

Elisabetta Vangelista

UK Debt Management Office

Abstract: This paper employs a Zero Lower Bound (ZLB) consistent shadow-rate model to decompose UK nominal yields into expectation and term premia components. Compared to a standard affine term structure model, it performs relatively better in a ZLB setting and effectively captures the countercyclical nature of term premia. The ZLB model is then exploited to estimate inflation expectations and risk premia. This entails jointly pricing and decomposing nominal and real UK yields. We find evidence that medium- and long-term inflation expectations are contained within narrower bounds since the early 1990s, suggesting monetary policy credibility improved after the introduction of inflation targeting.

Résumé: Ce papier utilise un modèle de taux d'intérêt virtuels (shadow-rate) cohérent avec la contrainte de la borne inferieur à zéro (ZLB) afin de décomposer les taux nominaux du Royaume-Uni en composantes d'anticipation et de prime de terme. Comparé à un modèle affine de structure par terme traditionnel, notre modèle shadow-rate est plus performant en période de ZLB et saisit la nature contra cyclique des primes de terme. Nous exploitons donc le modèle shadow-rate afin d'estimer des anticipations et des primes de risque d'inflation. Ceci consiste en la modélisation jointe des taux nominaux et réels du Royaume-Uni qui par la suite sont dcomposs. Nous trouvons que les anticipations d'inflation à moyen et long terme sont comprises dans des intervalles plus restreints depuis le début des années 1990, suggérant donc une amélioration de la crédibilité de la politique monétaire depuis l'adoption d'une cible d'inflation.

Non-technical summary

In an environment of very low nominal yield levels, central banks have been following closely inflation expectations measures. Those are available in many forms. Inflation expectations stemming from surveys are widely used but have the inconvenience of being scarcely available and of including few horizons. In addition Break-Even Inflation (BEI) rates, defined as the difference between nominal and real yields, provide policymakers with market expectations of future inflation levels. Nonetheless, assuming conventional and index-linked gilts are equally liquid; this measure is an imperfect representation of inflation expectations as it is polluted by an inflation risk premium. Nonetheless, aside from surveys and financial data, there is a third way of extracting inflation expectations, via term structure modeling.

The objective of this paper is to propose measures of inflation expectations and inflation risk premia through term structure decompositions. To this end, we need to build a model which allows the joint pricing of nominal and real yields. This model has to match adequately both nominal and real yields stylized facts. Some traditional models allow for the pricing of nominal and/or real yields. All these models belong to the affine Gaussian class of term structure models.

However, since the recent financial crisis, the behavior of the term structure of nominal yields has changed. Nominal yields, unlike real yields are now bound by the Zero Lower Bound (ZLB) and short-maturity yields have seen their volatility being compressed. These considerations lead to question the relevance of standard affine Gaussian term structure models as the expectations implied by these models might be violating the inherent asymmetry of nominal yields. Indeed, these models can generate, on the one hand, implausible nominal risk premia, and, imprecise future long-term expected inflation projections, on the other hand. Therefore, it becomes of crucial importance to refine these models and equip them with the ability to restrain nominal yields. Affine Gaussian term structure models are further unable to replicate the new feature of short-term rates being close to zero for prolonged periods of time, due to their fast reversion to the mean.

The recent literature has attempted tackling the ZLB constraint by straying away from affine Gaussian term structure models. Recent papers have thus responded to the ZLB constraint by proposing new models for the pricing of nominal yields. The most popular method involves the use of shadow-rate models, pioneered by Black (1995). To summarize, with the use of the properties of bond option pricing, it is now possible to uncover the non-linear relationship between prices, yields, and volatilities, and to price convexity effects in short maturity rates.

This paper considers two main issues. First, it aims at analyzing whether traditional models produce different results than ZLB-consistent models. Second, it provides decompositions of the term structure which allow us to assert the response of inflation expectations and inflation risk premia.

Our methodology consists in using the Christensen and Rudebusch (2015) shadow-rate model given its flexibility, simplicity and its ability to generate nominal yield and term premia estimates which are consistent with the ZLB constraint. Our contribution is to extend their shadow-rate to allow for the joint pricing of conventional and indexed-linked gilts such that only nominal yields are bound to be non-negative while real yields are left unconstrained. As far as future inflation projections are concerned, the benefits of using a no-arbitrage model come into play by enabling the disentanglement of inflation risk premia from BEI rates, thus providing estimates of pure inflation expectations (leaving aside liquidity premia).

2

We choose to work on the UK (1986-2014) because i) it is an economy that has been at the ZLB since March 2009. Moreover, many interesting policy events take place during our sample period, including the introduction of inflation targeting, the Bank of England independence, the reach of the ZLB as well as the the introduction of unconventional monetary policy in 2009; ii) Despite these interesting features of the UK economy, few papers have worked on the UK.

To our knowledge, our paper is the first that builds a ZLB consistent joint pricing model for nominal and real yields. Our analysis of UK yield curves from January 1986 to August 2014 indicates that traditional and ZLB-consistent models generate different results at the ZLB. Compared to a standard affine term structure model, a ZLB-consistent model performs relatively better in a ZLB setting and effectively captures the countercyclical nature of term premia. The ZLB model is then exploited to estimate inflation expectations and risk premia. This entails jointly pricing and decomposing nominal and real UK yields using a joint shadow-rate model that restricts nominal yields to be non-negative whilst allowing real rates to be unconstrained. Moreover inflation expectation and inflation risk premia are found to have strongly decreased after the introduction of inflation targeting and the independence of the Bank of England.

1. Introduction

In March 2009, the Monetary Policy Committee announced a cut of the policy rate to 0.5%, from a level of 4.5% six months earlier. This decision was accompanied by an economic stimulus amounting to a running total of £375bn. Since 2009, UK short yields stemming from conventional and index-linked gilts reached historically low levels.[1]

These considerations lead to question the use of standard affine Gaussian dynamic term structure models as the expectations implied by these models might be violating the inherent asymmetry of nominal yields. As a result, these models can generate, on the one hand, implausible nominal risk premia (as seen in Kim and Singleton (2012)), and on the other hand, imprecise future long-term expected inflation projections. Thus, it becomes of crucial importance to refine these models and equip them with the ability to restrain nominal yields.

In recent years, many models circumventing this issue have been proposed. Those include shadow-rate models, Gaussian quadratic models, square-root processes as well as AutoRegressive Gamma (ARG) zero processes.[2]

In addition to very low nominal yield levels, policymakers have also been preoccupied by inflation expectations. Break-Even Inflation (BEI) rates [3] provide policymakers with market expectations of future inflation levels. Nonetheless, assuming conventional and index-linked gilts are equally liquid, this measure is an imperfect representation of inflation expectations as it is polluted by an inflation risk premium.

This paper considers two main issues. First, it aims at analyzing whether traditional models produce different results than ZLB-consistent models. Second, it provides decompositions of the UK term structure which allow us to assert the response of inflation expectations and inflation risk premia.

We address both these issues by using the model recently proposed by Christensen and Rudebusch (2013a), which builds on Black (1995)'s and Krippner (2012)'s shadow rate framework. The model is a shadow-rate Arbitrage-Free Nelson Siegel (AFNS) term

---

[1]Negative nominal yields remain a possibility in periods of crisis, when bondholders require an insurance to safe-guard their investments, however it seems that an effective lower bound does exist and is a by-product of the level of the policy rate and the convenience yield.

[2]The latter, proposed by Monfort et al. (2015), develops a conditional distribution with zero point mass which allows a ZLB-consistent closed-form pricing of bonds.

[3]Defined as the difference between nominal and real yields.

structure model that imposes the non-negativity of interest rates. Unlike Kim and Singleton (2012)'s model, this particular representation has the benefit of being capable of encompassing more than two factors, concurrently preserving the simplicity of standard Gaussian models. Additionally, the factor loadings, borrowed from Nelson and Siegel (1987)'s model, facilitate the tractability of the no-arbitrage model and offer a reasonable interpretation of level, slope and curvature to the factors.

Our methodological contribution is to extend the shadow-rate model to allow for the joint pricing of conventional and indexed-linked gilts such that only nominal yields are bound to be non-negative. As far as future inflation projections are concerned, the benefits of using a no-arbitrage model come into play by enabling the disentanglement of inflation risk premia from BEI rates, thus providing estimates of pure inflation expectations.

In recent years, there have been a considerable number of papers examining inflation expectations and risk premia using affine models (see Chen et al. (2005), Christensen et al. (2010), D'Amico et al. (2010), Chun (2011), Chernov and Mueller (2012), Grishchenko and Huang (2012) and Hordahl and Tristani (2014)). However, limited literature is available for UK yields, despite the fact that the UK linker market is one of the most liquid ones and the UK Debt Management Office - an Executive Agency of HM Treasury - is committed to maintain this liquidity with regular issuance of inflation-linked bonds. A few exceptions include Joyce et al. (2010) that study UK inflation using affine models. Specifically, they obtain inflation projections up to 2009, thus before unconventional monetary policies were put in place. Similarly, Abrahams et al. (2015) use an affine term structure for the joint pricing of nominal and real yields that accounts for illiquidity on US and UK data.

Our analysis of UK yield curves from January 1986 to August 2014 indicates that traditional and ZLB-consistent models generate different results at the ZLB. Compared to a standard affine term structure model, a ZLB-consistent model performs relatively better in a ZLB setting and effectively captures the countercyclical nature of term premia. The ZLB model is then exploited to estimate inflation expectations and risk premia. This entails jointly pricing and decomposing nominal and real UK yields using a joint shadow-rate model that restricts nominal yields to be non-negative whilst allowing real rates to be unconstrained.

The paper is structured as follows. In Section 2 we estimate individual models, partic-

ularly, an AFNS model enforcing non-negativity for nominal yields and a standard AFNS model for real yields. In Section 3 we estimate a joint term structure model of nominal and real curves using an AFNS model that restricts solely nominal yields in a positive domain. No-arbitrage conditions allow us to further decompose BEI rates into two components, inflation risk premia and expectations, which can be found in Section 4. We provide concluding remarks in Section 5. An appendix provides further details on the derivation of the instantaneous forward rate and the extended Kalman filter.

2. Empirical affine models for nominal and real yields

This Section aims at comparing the fit of the standard AFNS model and its ZLB-consistent counterpart as well as the behaviour of nominal yields' decompositions, namely the expectation and term premium components. The findings incline us to support the use of shadow-rate models in fitting nominal yields at the ZLB. Furthermore, we estimate a standard AFNS model on real yields. These individual estimations on nominal and real yields are essential in the construction of the joint model. More particularly, the choice of the number and selection of the factors highly relies on these results.

2.1. Shadow-rate AFNS model for nominal yields

This Section discusses the estimation of standard (Gaussian) and shadow-rate AFNS models, and provides a comparison of the results obtained using nominal zero-coupon UK yields. The data set consists of continuously-compounded monthly nominal yields spanning from October 1986 to August 2014 and includes a set of seven maturities, namely 6, 12, 24, 36, 60, 84 and 120 months.[4] Interestingly, the time period incorporates three main changes in monetary policy practices in the UK: the introduction of inflation targeting in September 1992, the Bank of England's independence in May 1997, and the introduction of 'Quantitative Easing' in March 2009.

Before proceeding to the estimation, we need to go through two preliminary stages to best specify our model. First, we conduct a principal components analysis (PCA) to determine how many pricing factors are required to explain the cross-sectional variation

---

[4]The UK DMO issues bonds that have maturities of up to around 55 years. The aim of this study is to only analyse rate dynamics from short to medium horizons.

of nominal yields. Second, we use a general-to-specific method in order to impose the relevant restrictions to our model.

Table 1 displays the loadings from the principal components analysis for the set of maturities and the percentage of variation of yields that is being captured by each component. We notice that the first component is characteristic of a level factor due to its homogeneity, the second component incorporates a sign switch between shorter and longer maturities hence displaying a slope feature and finally the third component, being parabolic, has the behaviour of a curvature factor. Additionally, the first three components explain 99.99% of the cross-sectional yield variation. The PCA results validate our use of three factors bearing the interpretation of level, slope and curvature.

We use the three factor AFNS model proposed by Christensen et al. (2011). The latent state variables given by $X_t^N = \left(L_t^N, S_t^N, C_t^N \right)'$ solve the following system of stochastic differential equations under the risk-neutral $\mathbb{Q}$ measure, where λ^N is the mean reversion parameter, $W_t^{\mathbb{Q}}$ denotes a three dimensional Wiener process and the diffusion is diagonal.

$$
\begin{pmatrix} dL_t^N \\ dS_t^N \\ dC_t^N \end{pmatrix} = - \begin{pmatrix} 0 & 0 & 0 \\ 0 & \lambda^N & -\lambda^N \\ 0 & 0 & \lambda^N \end{pmatrix} \begin{pmatrix} L_t^N \\ S_t^N \\ C_t^N \end{pmatrix} dt + \begin{pmatrix} \sigma_{11,N} & 0 & 0 \\ 0 & \sigma_{22,N} & 0 \\ 0 & 0 & \sigma_{33,N} \end{pmatrix} \begin{pmatrix} dW_t^{L^N,\mathbb{Q}} \\ dW_t^{S^N,\mathbb{Q}} \\ dW_t^{C^N,\mathbb{Q}} \end{pmatrix} \quad (1)
$$

The instantaneous risk-free rate is an affine function of the state variables and is specifically defined as the sum of the level and slope factors:

$$
r_t^N = L_t^N + S_t^N. \quad (2)
$$

As shown in e.g. Ang and Piazzesi (2003), nominal zero-coupon bond prices are exponentially affine functions of the state variables. As an immediate consequence, the representation of nominal zero-coupon yields with maturity T at time t is given by an

affine function of the state variables, as shown below.

$$
\begin{aligned}
y^N(t,T) &= -\frac{A^N(t,T)}{T-t} - \frac{B^N(t,T)'}{T-t}X_t^N \\
&= L_t^N + \left(\frac{1-e^{-\lambda^N(T-t)}}{\lambda^N(T-t)}\right)S_t^N + \left(\frac{1-e^{-\lambda^N(T-t)}}{\lambda^N(T-t)} - e^{-\lambda^N(T-t)}\right)C_t^N - \frac{A^N(t,T)}{T-t},
\end{aligned}
\tag{3}
$$

where $A^N(t,T)$ and $B^N(t,T)$ are the unique solutions to a system of Riccati equations. $A^N(t,T)$ is known as the adjustment term (see Christensen et al. (2011) for the derivation) and $B^N(t,T)$ matches the Nelson-Siegel factor loadings.

The AFNS model is formulated in continuous time and Girsanov's theorem ensures the change from the physical to the risk-neutral measure, as such, $dW_t^{\mathbb{Q}} = dW_t^{\mathbb{P}} + \Gamma_t^N dt$, where Γ_t^N is the market price of risk and under essentially affine risk premium specifications (see Duffee (2002) and Cheridito et al. (2007)), it takes the form below, with γ_0^N being a three-dimensional vector and γ_1^N a 3x3 matrix:

$$
\Gamma_t^N = \gamma_0^N + \gamma_1^N X_t^N.
\tag{4}
$$

Having all the tools necessary, we can now extract the latent state variables $X_t^N = \left(L_t^N, S_t^N, C_t^N\right)'$ under the physical measure. The key parameters are $\kappa^{N,\mathbb{P}}$ and $\theta^{N,\mathbb{P}}$ which are unrestricted and σ^N which has a diagonal structure. The dynamics are given by the following stochastic differential equation:

$$
dX_t^N = \kappa^{N,\mathbb{P}}(t)\left[\theta^{N,\mathbb{P}}(t) - X_t^N\right]dt + \sigma^N dW_t^{X^N,\mathbb{P}}.
\tag{5}
$$

It is at this point that the general-to-specific strategy comes into play, as we implement it to find the best specification for the $\kappa^{N,\mathbb{P}}$ matrix. The procedure goes as follows. First, we estimate an unrestricted AFNS and set the least significant element of $\kappa^{N,\mathbb{P}}$ to zero. We then re-estimate the model with this restriction imposed, and so forth. At each iteration, we compute the Akaike Information Criterion (AIC) and Bayes Information Criterion. We repeat this process until we are left with a diagonal $\kappa^{N,\mathbb{P}}$. Both the AIC and BIC are provided on Table 2, and we will rule our decision by minimizing the AIC (when the

8

AIC and BIC decision rules do not coincide). The preferred specification is thus given by specification 6 in the Table, which is consistent with Christensen and Rudebusch (2012)'s findings. Table 3 and Table 4 indicate the parameter estimates and fit of the model, respectively.

Having estimated the standard AFNS model, we move on to the implementation of the shadow-rate AFNS which restricts nominal yields in the positive domain. The most striking difference will stem from the introduction of a shadow-rate which will have the same dynamics as the instantaneous risk-free rate under the standard AFNS, whilst the new dynamics for the instantaneous rate will consist of the maximum between the shadow-rate and zero [5]. The latent shadow-rates and instantaneous rates are respectively defined as:

$$s_t^N = L_t^N + S_t^N, \tag{6}$$

$$\underline{r}_t^N = max\left\{0, s_t^N\right\}. \tag{7}$$

As in the standard AFNS, the state dynamics under the risk-neutral $\mathbb{Q}$ measure and the physical $\mathbb{P}$ measure are given by equation (1) and (5), respectively. We will now use a few important concepts borrowed from the bond option price literature. Recently, Krippner (2012) developed a shadow-rate framework in which a representation for the Zero Lower Bound (ZLB) instantaneous forward rate is provided. This representation is valid for all Gaussian models, including the AFNS, and depends on the instantaneous forward shadow-rates as well as an additional component which is a function of the conditional variance of a European call. In the case of the shadow-rate AFNS, analytical solutions for the instantaneous forward shadow-rates and the conditional variance are provided by Christensen and Rudebusch (2013a). Their results can be found in the Appendix. Let us now denote by $\underline{y}^N(t, T)$, the Zero Lower Bound (ZLB) zero-coupon bond yields. In the

---

[5]The same analysis can be conducted with a different threshold. Recent developments in Denmark and Switzerland have shown that despite the existence of physical cash, interest rates can go negative; nonetheless, rates seem to be bound below by a threshold known as the convenience yield. In the case of the UK, we opt for zero (rather than 50 basis points which is the current bank rate level) as we want to reflect an "effective" lower bound for the UK that accounts for the convenience yield as well as the possibility of future downward revisions of the policy rate.

Appendix, we derive the following expression for $\underline{y}^N(t,T)$.[6]

$$\underline{y}^N(t,T) = \frac{1}{T-t} \int_t^T \left[f(t,s)\Phi\left(\frac{f(t,s)}{\omega(t,s)}\right) + \omega(t,s)\frac{1}{\sqrt{2\pi}}exp\left(-\frac{1}{2}\left[\frac{f(t,s)}{\omega(t,s)}\right]^2\right)\right] ds \quad (8)$$

It is important to note at this stage that $\underline{y}(t,T)$ is no longer a linear function of the state variables, unlike in the standard AFNS model. This non-linearity is translated in the estimation procedure, whereby a conventional Kalman Filter cannot be used and is replaced by an Extended Kalman Filter.[7]

We then apply the same general-to-specific strategy to this specification. The results of the general-to-specific method applied to the shadow-rate AFNS model are found on Table 5 and indicate that the preferred specification is thus given by specification (5). As in the standard AFNS case, the change of measure $dW_t^{\mathbb{Q}} = dW_t^{\mathbb{P}} + \Gamma_t^N dt$ combined with the essentially affine specification of risk $\Gamma_t^N = \gamma_0^N + \gamma_1^N X_t^N$ allow us to have the preferred specification's representation of the state dynamics under the physical measure:

$$\begin{pmatrix} dL_t^N \\ dS_t^N \\ dC_t^N \end{pmatrix} = \begin{pmatrix} \kappa_{11}^{N,\mathbb{P}} & 0 & 0 \\ \kappa_{21}^{N,\mathbb{P}} & \kappa_{22}^{N,\mathbb{P}} & \kappa_{23}^{N,\mathbb{P}} \\ 0 & 0 & \kappa_{33}^{N,\mathbb{P}} \end{pmatrix}\left[\begin{pmatrix} \theta_t^{L^N,\mathbb{P}} \\ \theta_t^{S^N,\mathbb{P}} \\ \theta_t^{C^N,\mathbb{P}} \end{pmatrix} - \begin{pmatrix} L_t^N \\ S_t^N \\ C_t^N \end{pmatrix}\right] dt + \begin{pmatrix} \sigma_{11,N} & 0 & 0 \\ 0 & \sigma_{22,N} & 0 \\ 0 & 0 & \sigma_{33,N} \end{pmatrix}\begin{pmatrix} dW_t^{L^N,\mathbb{P}} \\ dW_t^{S^N,\mathbb{P}} \\ dW_t^{C^N,\mathbb{P}} \end{pmatrix}.$$
$$(9)$$

The results of the estimated parameters can be found in Table 6, whilst the in-sample fit results, in Table 7, report a good fit for all maturities, particularly for medium-term maturities. The in-sample fit is comparable to the one obtained using a standard AFNS model and we do observe an improvement of roughly two basis points in the long-end of the curve. However, straying away from the performance throughout the entire sample and focusing only the ZLB period, our findings indicate that the ZLB-consistent model performs better than the traditional model. These findings reaffirm recent claims that shadow-rate models feature a superior performance (both in-sample and out-of-sample) during the ZLB, relative to standard affine and quadratic term structure models (see Christensen and Rudebusch (2013b), Kim and Priebsch (2013), Andreasen and Meldrum

---

[6]This is done by setting the vector $(X_1, X_2, X_3)'$ found in the Appendix equal to $(L_t^N, S_t^N, C_t^N)'$ and the variables $(\sigma_{11}, \sigma_{22}, \sigma_{33})$ equal to $(\sigma_{11,N}, \sigma_{22,N}, \sigma_{33,N})$.

[7]Alternatives to that procedure are the Iterated Extended Kalman Filter and the Unscented Kalman Filter, however the use of the Extended Kalman Filter is rather conventional in this literature.

(2014) and Bauer and Rudebusch (2014)). Moreover, it is important to stress that the log-likelihood of the ZLB-consistent model is higher for all specifications (including the preferred specification), providing further evidence in favour of this specification.

Figure 1 displays the state variables, namely the level, slope and curvature, estimated with the AFNS and shadow-rate AFNS models, respectively. The Figure shows that prior to the ZLB period state variables stemming from the two models roughly coincide and have a correlation of approximately 0.99. During the ZLB, this feature persists for both the level and the slope; however the curvature factor exhibits a significant change in behaviour from one model to another, with the correlation now dropping to roughly 0.84. This could be explained by the fact that the ZLB imposes a non-linear restriction, which potentially is best translated into effects on the non-linear curvature state variable.

Nominal yields are further decomposed into two components: the so called risk-neutral yields and the term premia. The latter can be computed through numerical methods and given by:

$$TP^N(t,T) = \underline{y}^N(t,T) - \frac{1}{T-t} \int_t^T \mathbb{E}_t^{\mathbb{P}} \left[\underline{r}_s^N \right] ds. \tag{10}$$

In Panel (a) of Figure 2, we provide estimates of the 10-year fitted term premia of nominal yields, with and without the ZLB assumption. At first glance, we notice the two series do not coincide even prior to the ZLB period. This finding is consistent with a similar comparison conducted by Ichiue and Ueno (2013). This difference can be justified by the highly sensitive nature of term premia to different preferred specifications used by each of these models. More importantly, prior to the ZLB, both term premia track each other and move in the same direction. Conversely, in recent years, models neglecting the ZLB restriction tend to underestimate term premia. With the ZLB specification, term premia now display a countercyclical nature, after 2009, thus corroborating Malik and Meldrum (2014)'s result whereby UK bond term premia are positively related to uncertainty about future inflation. It is interesting to note that the correlation between the two term premia prior to 2009 is equal to 0.99 while after 2009 this correlation drops to 0.85, which gives rise to the belief that at the ZLB, the curvature factor is of particular importance. In order to assess the effect of the incorporation of the ZLB in the model on expectations, in Panel (b) of Figure 2 we plot the expectation components of the ten-year

nominal yield obtained using a Gaussian and shadow-rate model. We observe that models neglecting the ZLB restriction tend to overestimate the fitted expectation term of the ten-year yield by up to 1%. This is consistent with Christensen and Rudebusch (2012)'s result which states that declines in US treasury yields mainly reflect lower expectations; however our result is at odds with their finding that declines in UK yields reflect reduced term premium. Our results indicate that term premia have maintained a countercyclical behaviour.[8]Moreover, it is worth mentioning that the expectation component under the Gaussian model is typically higher than under the shadow-rate model due to the fact that Gaussian models have a tendency to revert back to the mean relatively fast. In contrast, shadow-rate models are designed to maintain model-implied yields and their expectation terms relatively low for prolonged periods of time.

In order to assess how binding the ZLB is, in Figure 3 we depict the shadow-rate process. The latter displays a strong negativity after 2009, often reaching levels of -1%; thus supporting the use of a ZLB-consistent model. It is widely suggested in the literature that strongly negative shadow-rates may be interpreted as a largely accommodative stance of the central bank.

The constraint posed by the ZLB is also evident in forward rates. As an example we consider forward rates and risk-neutral expected short-rates at two different dates: the first date is June 2012, where the shadow-rate is at its lowest and the second date is August 2014 which is the last date of our sample. This will enable us to understand how forward rates respond relative to risk-neutral expected short-rates as the ZLB becomes less binding. Figure 4 plots the one year maturity forward and risk-neutral expected forward rates along with the shadow rate, in June 2012 (when the ZLB restriction is binding) and August 2014 (when the ZLB restriction is no longer binding), respectively. It is clear that the omission of the ZLB assumption can generate negative nominal short yields at times where the ZLB restriction is binding. As noted earlier, market demand can drive short maturity yields to negative territories, especially if bonds are perceived by investors as a

---

[8]The countercyclicality of risk premia paired with the fact that they increase with maturity suggest that in times of a recession - below trend growth -, issuing more short maturity bonds and rolling them over is likely to be more cost effective over the long horizon than issuing long maturity bonds. On the other hand, when the economy is in expansion, it could become more favorable to issue longer maturity bonds, as the premium paid to investors, relative to short maturity bonds, is lower, and the hedging of refinancing risk is cheaper on a relative scale.

'safe haven'. However, a prolonged period of negative short nominal rates, or equivalently, a negative policy rate, might not be reasonable for monetary policy objectives and would result in price tensions in market dynamics. Here, we note that shadow rates can turn significantly negative when modeled using the standard linear Gaussian AFNS mapping. What is observed in reality is that short rates are rather anchored at zero, hence capping the theoretical price of a zero coupon bond at 100 (see Krippner (2012)). If short rates were to go negative (Gaussian assumption), the price of a theoretical zero coupon bond ('shadow bond') would float anywhere above par. To summarise, with the use of the properties of bond option pricing, it is now possible to uncover the non-linear relationship between prices, yields, and volatilities, and to price convexity effects in short maturity rates. This relationship becomes evident when rates are at the zero lower bound and the option is in/at the money.[9]

2.2. Empirical AFNS model for real yields

We now proceed to the estimation of a standard AFNS model for real zero-coupon UK bond yields. The data set consists of continuously-compounded monthly yields spanning from October 1986 to August 2014 and includes a set of six fixed maturities: 60, 72, 84, 96, 108 and 120 months. It is important to note that we have chosen longer maturities for real yields, in comparison to nominal yields, due to a reduced liquidity of index-linked bonds in the short-end.

Table 8 displays the results of a principal components analysis on the set of real yields. It is clear that the first principal component that bears attributes of a level factor, explains a greater cross-sectional variation in real yields, in contrast to the case of nominal yields. One could argue that 2 factors suffice in the modelling of this set of real yields given they explain 99.99% of the variation. However, we take a closer look at the third component and notice that the typical U-shaped behaviour of a curvature factor persists. Moreover, our ultimate goal lies in estimating long term inflation expectations and it is common knowledge that the curvature factor is of high importance to longer maturity yields. Hence these two arguments justify our choice of using a three-factor AFNS model to fit real yields.

---

[9]Moneyness is the difference between strike price and future expected price. If the option is significantly in the money, the shadow bond price is well above par.

More importantly, it is crucial to identify that the second component bears a positive sign for shorter maturities and a negative sign for longer maturities, indicating the UK real yield curve has been inverted.

We denote by $X_t^R = \left(L_t^R, S_t^R, C_t^R\right)'$, the latent state variables. Under the risk-neutral measure $\mathbb{Q}$, where λ^R is the mean reversion parameter, $W_t^{\mathbb{Q}}$ denotes a three dimensional Wiener process and the diffusion is diagonal, the state dynamics are given by the following system of stochastic differential equations:

$$
\begin{pmatrix} dL_t^R \\ dS_t^R \\ dC_t^R \end{pmatrix} = - \begin{pmatrix} 0 & 0 & 0 \\ 0 & \lambda^R & -\lambda^R \\ 0 & 0 & \lambda^R \end{pmatrix} \begin{pmatrix} L_t^R \\ S_t^R \\ C_t^R \end{pmatrix} dt + \begin{pmatrix} \sigma_{11,R} & 0 & 0 \\ 0 & \sigma_{22,R} & 0 \\ 0 & 0 & \sigma_{33,R} \end{pmatrix} \begin{pmatrix} dW_t^{L^R,\mathbb{Q}} \\ dW_t^{S^R,\mathbb{Q}} \\ dW_t^{C^R,\mathbb{Q}} \end{pmatrix}. \tag{11}
$$

The instantaneous risk-free real rate is an affine function of the state variables and is defined as the sum of the level and slope factors:

$$
r_t^R = L_t^R + S_t^R. \tag{12}
$$

Real zero-coupon bond yields have the following structure, where $A^R(t,T)$ is the adjustment term and $B^R(t,T)$ are the Nelson Siegel loadings:

$$
\begin{aligned}
y^R(t,T) &= -\frac{A^R(t,T)}{T-t} - \frac{B^R(t,T)'}{T-t} X_t^R \\
&= L_t^R + \left(\frac{1-e^{-\lambda^R(T-t)}}{\lambda^R(T-t)}\right) S_t^R + \left(\frac{1-e^{-\lambda^R(T-t)}}{\lambda^R(T-t)} - e^{-\lambda^R(T-t)}\right) C_t^R - \frac{A^R(t,T)}{T-t}.
\end{aligned} \tag{13}
$$

Exactly as in the nominal case, the market price of risk takes an essentially affine specification seen below:

$$
dW_t^{\mathbb{Q}} = dW_t^{\mathbb{P}} + \Gamma_t^R dt, \tag{14}
$$

$$
\Gamma_t^R = \gamma_0^R + \gamma_1^R X_t^R. \tag{15}
$$

We can now apply the change of measure to obtain the latent state variables $X_t^R = \left(L_t^R, S_t^R, C_t^R\right)'$ under the physical measure. The key parameters are $\kappa^{R,\mathbb{P}}$ and $\theta^{R,\mathbb{P}}$ which

are unrestricted and σ^R which has a diagonal structure.

$$dX_t^R = \kappa^{R,\mathbb{P}}(t)\left[\theta^{R,\mathbb{P}}(t) - X_t^R\right]dt + \sigma^R dW_t^{X^R,\mathbb{P}} \tag{16}$$

Considering the fact that we use a three-factor AFNS model to fit real yields which, at first glance, do not seem to necessitate so many factors, it is very likely that some parameters may not be statistically significant. To accommodate for this possibility, we use a general-to-specific method, as before, to find the optimal specification of the $\kappa^{R,\mathbb{P}}$ matrix. The results -reported in Table 9- indicate that the diagonal specification (6) is the one that minimises both information criteria, and consequently is our preferred specification. The dynamics are given by the following stochastic differential equation:

$$\begin{pmatrix} dL_t^R \\ dS_t^R \\ dC_t^R \end{pmatrix} = \begin{pmatrix} \kappa_{11}^{R,\mathbb{P}} & 0 & \kappa_{13}^{R,\mathbb{P}} \\ 0 & \kappa_{22}^{R,\mathbb{P}} & 0 \\ 0 & 0 & \kappa_{33}^{R,\mathbb{P}} \end{pmatrix}\left[\begin{pmatrix} \theta_t^{L^R,\mathbb{P}} \\ \theta_t^{S^R,\mathbb{P}} \\ \theta_t^{C^R,\mathbb{P}} \end{pmatrix} - \begin{pmatrix} L_t^R \\ S_t^R \\ C_t^R \end{pmatrix}\right]dt + \begin{pmatrix} \sigma_{11,R} & 0 & 0 \\ 0 & \sigma_{22,R} & 0 \\ 0 & 0 & \sigma_{33,R} \end{pmatrix}\begin{pmatrix} dW_t^{L^R,\mathbb{P}} \\ dW_t^{S^R,\mathbb{P}} \\ dW_t^{C^R,\mathbb{P}} \end{pmatrix}. \tag{17}$$

The parameter estimates and in-sample fit can be found on Tables 10 and 11, respectively.

3. Empirical joint shadow-rate AFNS model for nominal and real yields

In this Section, we estimate a joint AFNS model for nominal and real yields. We impose the non-negativity assumption solely on nominal yields without restricting real yields. We consider a data set combining the two panels studied in the previous Section. Therefore, the data consists of continuously-compounded monthly nominal and real yields spanning from October 1986 to August 2014 and includes a set of seven maturities for nominal yields, namely, 6, 12, 24, 36, 60, 84 and 120 months, and an additional set of six maturities for real yields: 60, 72, 84, 96, 108 and 120 months.[10] Nonetheless, before proceeding to our joint

---

[10]The data set is provided by the DMO. In line with the Bank of England, Variable Roughness Penalty (VRP) estimates of nominal and real spot rates are computed following Anderson and Sleath (2001). However, unlike the Bank of England, the DMO does not use GC rates for the estimation of nominal VRP zero rates but only gilt data with maturity greater than 3 months. Further details regarding the data set are available upon request.

shadow-rate AFNS model, we need to establish the number of factors to be considered, as well as the interpretation we wish to give to these factors. To do so, we first perform a principal components analysis, results are displayed in Table 12. At first glance, we can see that the use of six factors would be somewhat of a stretch. By the same token, the use of three factors seems, a priori, far too restrictive to be able to fit the term structure of nominal and real yields appropriately. We now face the dilemma between using four or five factors. On the one hand, our nominal yields' data set includes short, medium and long term maturities, which implies the need for a level, slope and curvature factor. On the other hand, real yields comprise solely of medium and long term maturities, which ultimately give a greater weight to the level and curvature factors. One could hence argue that an appropriate model could have a level, slope and curvature for nominal yields, a curvature for real yields and finally a common level and slope factor, as it is the case in Christensen et al. (2010). However, this model would be unfeasible as it would violate the no-arbitrage assumption imposed on the AFNS model in order to retrieve the Nelson-Siegel factor loadings (see Christensen et al. (2009)). The assumption of no-arbitrage is os key to our approach, as it requires both the risk-neutral and physical measure in order to retrieve inflation risk premia. In addition, we find that, empirically, the correlation between long nominal and real yields, representing the level, has been historically very stable over time and that nominal yields moved very much in line with real yields, thus supporting the choice of using one single level factor to explain both nominal and real rates. We find that nominal and real rates' slopes, especially at 5 and 10-year maturities, also display a historically stable correlation, however, this pattern changes after 2008. This coincides with the timing of the sudden decrease in nominal rates and the significant increase in the steepness of the nominal curve, resulting in the sharp increase in BEI at 5 and 10-year maturities. In practice, if we were to use a single slope factor, we would misestimate the short real rate consequently also affecting inflation expectations after 2008. We therefore choose to use a five factor model which consists of an extension of the Svensson model. This model has the capacity to capture the inversion of real yields, by allowing their slope to vary independently from the slope of nominal yields. The first five principal components explain 99.99% of the cross-sectional variation of nominal and real yields, therefore the choice of five factors is reasonable. We are hence left with a single interpretation for our

factors, whereby the first three factors represent the level, slope and curvature of nominal yields, whilst the fourth and fifth factors represent the slope and curvature of real yields, respectively. By deduction, the level factor will be common across the two sets of yields. We denote by α^R the weight of real yields on the level of nominal yields.

As in the nominal case, before enforcing the zero lower-bound on nominal yields, we need to first find the preferred specification of our mean reversion matrix $\kappa^{J,\mathbb{P}}$. Using the so-called preferred specification is of great importance due to the sensitivity of results to different specifications (see Joslin et al. (2014), Joslin et al. (2011) and Christensen and Rudebusch (2013a)). The issue of sensitivity is of greater importance when considering the estimation of risk premia, given they rely heavily on the estimation of $\kappa^{J,\mathbb{P}}$. We hence proceed in conducting such a strategy on a joint shadow-rate AFNS model which imposes the non-negativity assumption solely on nominal yields [11].

We first consider the structure of our joint shadow-rate AFNS model. The joint latent state vector is given by $X_t^J = \left(L_t, S_t^N, C_t^N, S_t^R, C_t^R\right)'$ and solves the following stochastic differential equations under the risk-neutral measure $\mathbb{Q}$:

$$
\begin{pmatrix} dL_t \\ dS_t^N \\ dC_t^N \\ dS_t^R \\ dC_t^R \end{pmatrix} = - \begin{pmatrix} \epsilon & 0 & 0 & 0 & 0 \\ 0 & \lambda^N & -\lambda^N & 0 & 0 \\ 0 & 0 & \lambda^N & 0 & 0 \\ 0 & 0 & 0 & \lambda^R & -\lambda^R \\ 0 & 0 & 0 & 0 & \lambda^R \end{pmatrix} \begin{pmatrix} L_t \\ S_t^N \\ C_t^N \\ S_t^R \\ C_t^R \end{pmatrix} dt + \begin{pmatrix} \sigma_{11,J} & 0 & 0 & 0 & 0 \\ 0 & \sigma_{22,J} & 0 & 0 & 0 \\ 0 & 0 & \sigma_{33,J} & 0 & 0 \\ 0 & 0 & 0 & \sigma_{44,J} & 0 \\ 0 & 0 & 0 & 0 & \sigma_{55,J} \end{pmatrix} \begin{pmatrix} dW_t^{L,\mathbb{Q}} \\ dW_t^{S^N,\mathbb{Q}} \\ dW_t^{C^N,\mathbb{Q}} \\ dW_t^{S^R,\mathbb{Q}} \\ dW_t^{C^R,\mathbb{Q}} \end{pmatrix},
$$

(18)

where λ^N and λ^R are scalars that represent the speed of mean-reversion for nominal and real yields respectively, and $dW_t^{\mathbb{Q}}$ is a five-dimensional Wiener process.

The joint shadow-rate AFNS model restricts nominal yields in the positive domain whilst simultaneously keeping real yields unrestricted. The instantaneous risk-free nominal

---

[11]A similar analysis is conducted on a joint standard AFNS model. Results of the general-to-specific method, parameter estimates and fit of the model are available upon request

and real rates are thus given respectively by:

$$\underline{r}_t^N = max\left\{0, L_t + S_t^N\right\}, \tag{19}$$

$$r_t^R = \alpha^R L_t + S_t^R. \tag{20}$$

We note that the nominal instantaneous risk-free rate is the maximum between zero and the nominal shadow-rate, whilst the real instantaneous risk-free rate coincides with the fictif real shadow-rate. Let us now denote by $\underline{y}^N(t, T)$ and $y^R(t, T)$, the ZLB nominal zero-coupon bond yields and the real zero coupon yields, respectively. In the Appendix we derive $\underline{y}^N(t, T)$.[12] Their representations are given as follows:

$$\underline{y}^N(t, T) = \frac{1}{T-t}\int_t^T \left[f^N(t, s)\Phi\left(\frac{f^N(t, s)}{\omega^N(t, s)}\right) + \omega^N(t, s)\frac{1}{\sqrt{2\pi}}exp\left(-\frac{1}{2}\left[\frac{f^N(t, s)}{\omega_N(t, s)}\right]^2\right)\right]ds, \tag{21}$$

$$y^R(t, T) = \alpha^R L_t + \left(\frac{1 - e^{-\lambda^R \tau}}{\lambda^R \tau}\right)S_t^R + \left(\frac{1 - e^{-\lambda^R \tau}}{\lambda^R \tau} - e^{-\lambda^R \tau}\right)C_t^R - \frac{A^R(\tau)}{\tau}. \tag{22}$$

This model can be written in state-space representation and estimated through maximum likelihood. It is crucial to observe that nominal yields are non-linear functions of the state vector and real yields are affine function of the latent state variables. As a consequence, to accommodate for the non-linearity, the computation of the likelihood requires the use of an Extended Kalman Filter.

The market price of risk under the essentially affine risk premium specifications takes the form:

$$dW_t^{\mathbb{Q}} = dW_t^{\mathbb{P}} + \Gamma_t^J dt, \tag{23}$$

$$\Gamma_t^J = \gamma_0^J + \gamma_1^J X_t^J. \tag{24}$$

By applying the change of measure, we extract the latent state variable vector $X_t^J = \left(L_t, S_t^N, C_t^N, S_t^R, C_t^R\right)'$ which solves the stochastic differential equations below under the

---

[12]This is done by setting the vector $(X_1, X_2, X_3)'$ found in the Appendix equal to $(L_t, S_t^N, C_t^N)'$ and the variables $(\sigma_{11}, \sigma_{22}, \sigma_{33})$ equal to $(\sigma_{11,J}, \sigma_{22,J}, \sigma_{33,J})$.

physical measure:

$$dX_t^J = \kappa^{J,\mathbb{P}}(t)\left[\theta^{J,\mathbb{P}}(t) - X_t^J\right]dt + \sigma^J dW_t^{XJ,\mathbb{P}}. \tag{25}$$

We can now implement a general-to-specific method to find the best specification for the $\kappa^{J,\mathbb{P}}$ matrix. We first start by estimating an unrestricted model and continue by setting the least significant element of $\kappa^{J,\mathbb{P}}$ to zero. We then re-estimate the model with this restriction imposed, and so forth. This process is repeated until we are left with a diagonal $\kappa^{J,\mathbb{P}}$. For each step, the log-likelihood, AIC and BIC are reported in Table 13. We aim to minimise the information criteria, in this case the decision rule of the AIC and BIC coincide, and thus designate specification (21) as our preferred specification. The latent state variable $X_t^J = \left(L_t, S_t^N, C_t^N, S_t^R, C_t^R\right)'$ solves the following stochastic differential equation under the physical measure, for our preferred specification:

$$\begin{pmatrix} dL_t \\ dS_t^N \\ dC_t^N \\ dS_t^R \\ dC_t^R \end{pmatrix} = \begin{pmatrix} \kappa_{11}^{J,\mathbb{P}} & 0 & 0 & 0 & 0 \\ 0 & \kappa_{22}^{J,\mathbb{P}} & 0 & 0 & 0 \\ 0 & 0 & \kappa_{33}^{J,\mathbb{P}} & 0 & 0 \\ 0 & 0 & 0 & \kappa_{44}^{J,\mathbb{P}} & 0 \\ 0 & 0 & 0 & 0 & \kappa_{55}^{J,\mathbb{P}} \end{pmatrix} \left[\begin{pmatrix} \theta_t^L \\ \theta_t^{S^N} \\ \theta_t^{C^N} \\ \theta_t^{S^R} \\ \theta_t^{C^R} \end{pmatrix} - \begin{pmatrix} L_t \\ S_t^N \\ C_t^N \\ S_t^R \\ C_t^R \end{pmatrix} \right] dt + diag \begin{pmatrix} \sigma_{11,J} \\ \sigma_{22,J} \\ \sigma_{33,J} \\ \sigma_{44,J} \\ \sigma_{55,J} \end{pmatrix} \begin{pmatrix} dW_t^{L,\mathbb{P}} \\ dW_t^{S^N,\mathbb{P}} \\ dW_t^{C^N,\mathbb{P}} \\ dW_t^{S^R,\mathbb{P}} \\ dW_t^{C^R,\mathbb{P}} \end{pmatrix},$$

$$\tag{26}$$

The estimated parameters comprising the equation above are reported in Table 14 and the in-sample fit is displayed in Table 15. The findings under the joint model are consistent with the individual models' results. The fit of both nominal and real yields is very satisfactory and further allows us to explore, inflation expectations and risk premia, which we discuss in the next Section.

4. Inflation expectations and risk premia

In this Section we address the decomposition of BEI rates into inflation risk premia and expectations. The no-arbitrage condition so far imposed on all AFNS models gains further

importance in this Section as it is precisely the existence of a risk-neutral and physical measure that eventually provides us this decomposition. We denote by $\frac{dM_t^N}{M_t^N}$ and $\frac{dM_t^R}{M_t^R}$, the nominal and real pricing kernel dynamics, respectively, and provide their expressions below:

$$\frac{dM_t^N}{M_t^N} = -\underline{r}_s^N dt - \Gamma_t^{J'} dW_t^{J,\mathbb{P}}, \tag{27}$$

$$\frac{dM_t^R}{M_t^R} = -r_t^R dt - \Gamma_t^{J'} dW_t^{J,\mathbb{P}}. \tag{28}$$

By manipulating the two stochastic discount factors above, (see Christensen et al. (2010) for further details), one can extract the following system of equations:

$$BEI(t,T) \equiv \underline{y}_t^N(t,T) - y_t^R(t,T) \tag{29}$$

$$= \pi_t^e(t,T) + \phi_t(t,T), \tag{30}$$

$$\pi_t^e(t,T) = -\frac{1}{T-t} ln\left\{ \mathbb{E}_t^{\mathbb{P}}\left[exp\left(-\int_t^T (r_u^N - r_u^R)du \right) \right] \right\}, \tag{31}$$

where $\pi_t^e(t,T)$ and $\phi_t(t,T)$ denote respectively the inflation expectations and inflation risk premia for maturity T, estimated at time t. Moreover, the solution to the expression in curly brackets is obtained through numerical procedures. It is worth noting that $\pi_t^e(t,T)$ is implicitly a function of the common level factor as well as the two individual nominal and real slope factors and that it is a continuous process, hence it is not directly comparable to observed inflation.

In Panel (a) of Figure 5, we display the 5- and 10-year inflation expectations. We identify a handful of key monetary policy events over the sample, including the adoption of inflation targeting in September 1992 (sparked by the withdrawal of the pound sterling from the European Exchange Rate Mechanism), the independence of the Bank of England in setting monetary policy in May 1997, the cut of the bank rate to 0.5% and launch of the asset purchase programme in March 2009, the asset purchase programme reaching a running total of £375bn in July 2012 (thus amounting to roughly 30% of debt at the time), and finally forward guidance in August 2013 and February 2014. We note that since 1992 inflation expectations have decreased, possibly as a result of investors' confidence in the new monetary policy framework that was reinforced in the Bank of England Act 1998;

similar results are found in Joyce et al. (2010) and Andreasen (2012). Since the mid-2000s, there is a tendency for the 5- and 10-year spot inflation projections to be below the current inflation level, while at a 10-year horizon, inflation projections systematically undershoot target inflation after 2008.[13] In 2008, inflation expectations decreased significantly, perhaps overly so, relatively to the magnitude of change observed in CPI inflation thereafter. Historically, this occurred in conjunction with large volatility in the inflation-linked bond market, which suffered reduced liquidity. At that time, inflation-linked gilt asset swap spreads sharply widened to historical highs. As a result, it is possible that our estimation has been affected by this event and that inflation expectations and risk premia require an adjustment for liquidity premia, especially at longer horizons. Linkers are typically less liquid than conventional bonds of similar maturity. We tested the drop in 2008 against alternative data sources, including inflation survey forecast data.[14] Our results confirm the fall in 2008 is likely to be the product of a distortion in market prices. Subsequently to this sharp drop, expectations have picked up and have reached, once again, post-1997 average levels.

Panel (b) of Figure 5 depicts 5- and 10-year inflation risk premia. We observe that the compensation for inflation risk significantly dropped after the independence of the Bank of England, suggesting a gained credibility in inflation-targeting practices and conveying a period of lower uncertainty. Moreover, there are indications that the fall in term premia observed in Figure 2 might very well be driven by lower inflation risk premia during that period, whilst the sharp increase in inflation risk premia in the late 2008 is likely driven by liquidity and pricing distortions in the linker market. Though inflation premia dropped soon after March 2009, they have been steadily increasing since August 2013 as investors might have been placing more weight on future inflation uncertainty.

The dcomposition in Figure 5 is based on model-implied BEI rates. We now focus on actual BEI rates which allows us to evaluate the fit of the model. This is shown in Figure 6 where the 5- and 10-year actual BEI rates are decomposed into inflation expectations, inflation risk premia and a residual which represents the discrepancy between actual and

---

[13]We took into account that inflation expectations are RPI based since index-linked gilts differ from conventional gilts in that payments are adjusted in line with movements in RPI. It is worth mentioning that in December 2003, the Bank of England changed its inflation target from a 2.5% level of RPIX to a 2% level of CPI.

[14]From Consensus Economics.

model-implied BEI rates. The residuals being very close to zero provides evidence that our model fits well BEI rates.

5. Conclusion

This paper first examined how the performance of a standard AFNS model fairs against its shadow-rate model counterpart. Our findings indicate that accounting for the ZLB improves the in-sample goodness of fit of the estimated yields (in terms of RMSE) and allows replicating some of the stylized facts yields feature at the ZLB. In addition, it is found that the standard AFNS model overestimates the expectation term of yields, thus leading to an undershooting of term premia. In contrast, the shadow-rate AFNS model is able to feature a countercyclical nominal term premium.

Having argued for the superior performance of shadow-rate models at the ZLB (vis-à-vis standard Gaussian affine term structure models), we subsequently exploited this result to build a ZLB-consistent model that jointly prices nominal and real yields.

We specified and estimated a joint shadow-rate AFNS model that is able to impose the zero lower bound restriction on nominal yields whilst allowing real yields to fall below zero. The model proposed features benefits from the Nelson Siegel factor loadings which induce a robust estimation procedure and tractability. The no-arbitrage restrictions enhance the theoretical grounds whilst simultaneously allowing the decomposition of BEI rates into inflation expectations and risk premia. When estimated using UK data, the proposed model successfully fits both nominal and real yields as well as BEI rates.

We find that imposing the zero lower bound in the model specification allows to correct for the unreasonably low term premia projections stemming from a standard AFNS model after 2009.

Our decompositions provide evidence supporting the conclusion that the Bank of England Act 1998 established credibility in inflation-targeting. Finally, we find that inflation premia have been steadily increasing since August 2013, suggesting investors might be placing more weight on future inflation uncertainty.

Appendix A: Shadow-rate AFNS model à la Krippner

The instantaneous shadow forward rates are obtained by deriving the logarithmic bond prices P(t,T) with respect to the maturity T, as follows:

$$
\begin{aligned}
f(t,T) &= -\frac{\partial}{\partial T}lnP(t,T) \\
&= X_1 + e^{-\lambda(T-t)}X_2 + \lambda(T-t)e^{-\lambda(T-t)}X_3 + A^f(t,T),
\end{aligned}
\tag{32}
$$

where $A^f(t,T)$ is obtained below:

$$
\begin{aligned}
A^f(t,T) &= -\frac{\partial A(t,T)}{\partial T} \\
&= -\frac{1}{2}\sigma_{11}^2(T-t)^2 - \frac{1}{2}\sigma_{22}^2\left(\frac{1-e^{-\lambda(T-t)}}{\lambda}\right)^2 \\
&\quad - \frac{1}{2}\sigma_{33}^2\left((T-t)e^{-\lambda(T-t)} - \frac{1-e^{-\lambda(T-t)}}{\lambda}\right)^2.
\end{aligned}
\tag{33}
$$

We denote by $v(t,T,T+\epsilon)$ the conditional variance of a European call option maturing at time T, contingent on the zero-coupon bond with maturity $T+\epsilon$.

$$
\begin{aligned}
v(t,T,T+\epsilon) &= \sigma_{11}^2\epsilon^2(T-t) + \sigma_{22}^2\left(\frac{1-e^{-\lambda\epsilon}}{\lambda}\right)^2\frac{1-e^{-2\lambda(T-t)}}{2\lambda} + \sigma_{33}^2\left[\left(\frac{1-e^{-\lambda\epsilon}}{\lambda}\right)^2\frac{1-e^{-2\lambda(T-t)}}{2\lambda}\right.\\
&\quad + e^{-2\lambda\epsilon}\left[\frac{\epsilon^2-(T-t+\epsilon)^2e^{-2\lambda(T-t)}}{2\lambda} + \frac{\epsilon-(T-t+\epsilon)e^{-2\lambda(T-t)}}{2\lambda^2} + \frac{1-e^{-2\lambda(T-t)}}{4\lambda^3}\right]\\
&\quad - \frac{1}{2\lambda}(T-t)^2e^{-2\lambda(T-t)} - \frac{1}{2\lambda^2}(T-t)e^{-2\lambda(T-t)} + \frac{1-e^{-2\lambda(T-t)}}{4\lambda^3}\\
&\quad - \frac{\left(1-e^{-\lambda\epsilon}\right)e^{-\lambda\epsilon}}{\lambda^2}\left[\epsilon-(T-t+\epsilon)e^{-2\lambda(T-t)} + \frac{1-e^{-2\lambda(T-t)}}{2\lambda}\right]\\
&\quad + \frac{\left(1-e^{-\lambda\epsilon}\right)}{\lambda^2}\left[\frac{1-e^{-2\lambda(T-t)}}{2\lambda} - (T-t)e^{-2\lambda(T-t)}\right]\\
&\quad + \frac{\epsilon e^{-\lambda\epsilon}}{\lambda}\left[(T-t)e^{-2\lambda(T-t)} - \frac{1-e^{-2\lambda(T-t)}}{2\lambda}\right]\\
&\quad \left.+ \frac{\epsilon e^{-\lambda\epsilon}}{\lambda}\left[(T-t)^2e^{-2\lambda(T-t)} + \frac{1}{\lambda}(T-t)e^{-2\lambda(T-t)} - \frac{1-e^{-2\lambda(T-t)}}{2\lambda^2}\right]\right]
\end{aligned}
\tag{34}
$$

The conditional variance is further transformed to obtain a representation of $\omega(t,T)^2$:

$$
\begin{aligned}
\omega(t,T)^2 &= \frac{1}{2}\lim_{\epsilon\to 0}\frac{\partial^2 v(t,T,T+\epsilon)}{\partial\epsilon^2} \\
&= \sigma_{11}^2(T-t) + \sigma_{22}^2\left(\frac{1-e^{-2\lambda(T-t)}}{2\lambda}\right) \\
&\quad + \sigma_{33}^2\left[\frac{1-e^{-2\lambda(T-t)}}{4\lambda} - \frac{1}{2}(T-t)e^{-2\lambda(T-t)} - \frac{1}{2}\lambda(T-t)^2 e^{-2\lambda(T-t)}\right].
\end{aligned}
\tag{35}
$$

Let us now denote by $\underline{f}(t,T)$, the Zero Lower Bound (ZLB) instantaneous forward rate. Setting $\Phi(.)$ to be the standard normal cumulative probability, we obtain a representation for $\underline{f}(t,T)$:

$$
\underline{f}(t,T) = f(t,T)\Phi\left(\frac{f(t,T)}{\omega(t,T)}\right) + \omega(t,T)\frac{1}{\sqrt{2\pi}}exp\left(-\frac{1}{2}\left[\frac{f(t,T)}{\omega(t,T)}\right]^2\right).
\tag{36}
$$

Appendix B: Extended Kalman filter

The estimation of a shadow rate term structure model resembles the one of a Gaussian model in many ways. Specifically, the state equation of the state-space representation remains intact and the sole change in the algorithm stems from the non-linearity in the space equation. Therefore, rather than using a Kalman filter routine, an Extended Kalman filter is used, whereby the algorithm remains identical in all the steps that relate to the state equation, and the only change that occurs is to perform a Taylor expansion in order to approximate the space equation and linearize it.

First, let us disclose the details pertaining to the state equation, which are identical to the standard Kalman filter. Below is the transition equation in its discretized form.

$$
X_T = \left[I - exp(-\kappa^{\mathbb{P}}(T-t))\right]\theta^{\mathbb{P}} + exp(-\kappa^{\mathbb{P}}(T-t))X_t + \eta_t
\tag{37}
$$

The standard moments conditions are displayed below:

$$
\mathbb{E}^{\mathbb{P}}[X_T|\mathcal{F}_t] = \left[I - exp(-\kappa^{\mathbb{P}}(T-t))\right]\theta^{\mathbb{P}} + exp(-\kappa^{\mathbb{P}}(T-t))X_t,
\tag{38}
$$

$$
\mathbb{V}^{\mathbb{P}}[X_T|\mathcal{F}_t] = \int_t^T exp(-\kappa^{\mathbb{P}}(T-s))\Sigma\Sigma' exp(-\kappa^{\mathbb{P}'}(T-s))ds.
\tag{39}
$$

The initial conditions for the Extended Kalman filter are set to the unconditional mean and covariance matrix, given in equation (40) and (41), as in the standard case.

$$\hat{X}_0 = \theta^{\mathbb{P}} \tag{40}$$

$$\hat{\Sigma}_0 = \int_0^{\infty} exp(-\kappa^{\mathbb{P}}s)\Sigma\Sigma' exp(-\kappa^{\mathbb{P}'}s)ds \tag{41}$$

Now, proceeding to the differences that stem from the non-linearity of the measurement equation, let us denote by ψ the parameters of the model and assume the error terms η_t and ϵ_t are orthogonal and ϵ_t is i.i.d. The space equation can be written as follows, where the function k is non-linear.

$$y_t = k(X_t; \psi) + \epsilon_t \tag{42}$$

This equation is now linearized using a first-order Taylor expansion as shown below. The approximation is performed around the optimal guess of X_t within the prediction step of the algorithm, given by $X_{t|t-1}$.

$$k(X_t; \psi) \approx k(X_{t|t-1}; \psi) + \frac{\partial k(X_t; \psi)}{\partial X_t}|_{X_t = X_{t|t-1}}(X_t - X_{t|t-1}) \tag{43}$$

The space equation takes the following form:

$$y_t = \mathbb{A}_t(\psi) + \mathbb{B}_t(\psi)X_t + \epsilon_t. \tag{44}$$

where $\mathbb{A}_t(\psi)$ and $\mathbb{B}_t(\psi)$ are provided below.

$$\mathbb{A}_t(\psi) = k(X_{t|t-1}; \psi) - \frac{\partial k(X_t; \psi)}{\partial X_t}|_{X_t = X_{t|t-1}}X_{t|t-1} \tag{45}$$

$$\mathbb{B}_t(\psi) = \frac{\partial k(X_t; \psi)}{\partial X_t}|_{X_t = X_{t|t-1}} \tag{46}$$

References

Abrahams M, Adrian T, Crump RK, , Moench E. 2015. Decomposing real and nominal yield curves. Technical report, Federal Reserve Bank of New York.

Anderson N, Sleath J. 2001. New estimates of the UK real and nominal yield curves. Bank of England working papers 126, Bank of England.

Andreasen MM. 2012. An estimated DSGE model: Explaining variation in nominal term premia, real term premia, and inflation risk premia. *European Economic Review* **56**: 1656–1674.

Andreasen MM, Meldrum A. 2014. Dynamic term structure models: The best way to enforce the zero lower bound. Technical report, School of Economics and Management, University of Aarhus.

Ang A, Piazzesi M. 2003. A no-arbitrage vector autoregression of term structure dynamics with macroeconomic and latent variables. *Journal of Monetary Economics* **50**: 745–787.

Bauer MD, Rudebusch GD. 2014. Monetary policy expectations at the zero lower bound. Technical report, Federal Reserve Bank of San Francisco.

Black F. 1995. Interest rates as options. *The Journal of Finance* **50**: 1371–1376. ISSN 1540-6261.

Chen RR, Liu B, Cheng X. 2005. Inflation, fisher equation, and the term structure of inflation risk premia: Theory and evidence from tips .

Cheridito P, Filipovic D, Kimmel RL. 2007. Market price of risk specifications for affine models: Theory and evidence. *Journal of Financial Economics* **83**: 123–170.

Chernov M, Mueller P. 2012. The term structure of inflation expectations. *Journal of Financial Economics* **106**: 367–394.

Christensen JH, Diebold FX, Rudebusch GD. 2011. The affine arbitrage-free class of nelson-siegel term structure models. *Journal of Econometrics* **164**: 4–20.

Christensen JH, Rudebusch GD. 2012. The response of interest rates to u.s. and u.k. quantitative easing. *Economic Journal* **122**: F385–F414.

Christensen JH, Rudebusch GD. 2013a. Estimating shadow-rate term structure models with near-zero yields. Working Paper Series 2013-07, Federal Reserve Bank of San Francisco.

Christensen JH, Rudebusch GD. 2013b. Modeling yields at the zero lower bound: are shadow rates the solution? Technical Report 2013-39, Federal Reserve Bank of San Francisco.

Christensen JHE, Diebold FX, Rudebusch GD. 2009. An arbitrage-free generalized nelson–siegel term structure model. *Econometrics Journal* **12**: C33–C64.

Christensen JHE, Lopez JA, Rudebusch GD. 2010. Inflation expectations and risk premiums in an arbitrage-free model of nominal and real bond yields. *Journal of Money, Credit and Banking* **42**: 143–178.

Chun AL. 2011. Expectations, bond yields, and monetary policy. *Review of Financial Studies* **24**: 208–247.

D'Amico S, Kim DH, Wei M. 2010. Tips from tips: the informational content of treasury inflation-protected security prices. Finance and Economics Discussion Series 2010-19, Board of Governors of the Federal Reserve System (U.S.).

Duffee GR. 2002. Term premia and interest rate forecasts in affine models. *Journal of Finance* **57**: 405–443.

Grishchenko OV, Huang JZ. 2012. Inflation risk premium: evidence from the tips market. Finance and Economics Discussion Series 2012-06, Board of Governors of the Federal Reserve System (U.S.).

Hordahl P, Tristani O. 2014. Inflation risk premia in the us and the euro area. *Journal of the European Economic Association* **10**: 634–657.

Ichiue H, Ueno Y. 2013. Estimating Term Premia at the Zero Bound: An Analysis of

Japanese, US, and UK Yields. Bank of Japan Working Paper Series 13-E-8, Bank of Japan.

Joslin S, Priebsch M, Singleton KJ. 2014. Risk premiums in dynamic term structure models with unspanned macro risks. *Journal of Finance* **69**: 1197–1233.

Joslin S, Singleton KJ, Zhu H. 2011. A new perspective on gaussian dynamic term structure models. *Review of Financial Studies* **24**: 926–970.

Joyce MA, Lildholdt P, Sorensen S. 2010. Extracting inflation expectations and inflation risk premia from the term structure: A joint model of the uk nominal and real yield curves. *Journal of Banking & Finance* **34**: 281–294.

Kim DH, Priebsch MA. 2013. Estimation of multi-factor shadow-rate term structure models. Technical report, Board of Governors of the Federal Reserve System (U.S.).

Kim DH, Singleton KJ. 2012. Term structure models and the zero bound: An empirical investigation of japanese yields. *Journal of Econometrics* **170**: 32 – 49. ISSN 0304-4076.

Krippner L. 2012. Modifying gaussian term structure models when interest rates are near the zero lower bound. Reserve Bank of New Zealand Discussion Paper Series DP2012/02, Reserve Bank of New Zealand.

Malik S, Meldrum A. 2014. Evaluating the robustness of UK term structure decompositions using linear regression methods. Bank of England working papers 518, Bank of England.

Monfort A, Pegoraro F, Renne JP, Roussellet G. 2015. Staying at zero with affine processes: An application to term-structure modelling. Technical report, Paris December 2014 Finance Meeting EUROFIDAI - AFFI Paper.

Nelson CR, Siegel AF. 1987. Parsimonious modeling of yield curves. *The Journal of Business* **60**: 473–89.

Table 1: First three principal components in nominal yields.

Maturity	First PC	Second PC	Third PC
6 months	0.4212	-0.4861	0.5232
12 months	0.4120	-0.3699	0.0981
24 months	0.3971	-0.1723	-0.3303
36 months	0.3841	-0.0029	-0.4839
60 months	0.3622	0.2596	-0.3315
84 months	0.3428	0.4339	0.0451
120 months	0.3146	0.5844	0.5113
% explained	97.90	1.95	0.14

NOTE: We provide the loadings of the yields of the set of maturities on the first three principal components. The percentage of all nominal bond yields' cross-sectional variation accounted for by each component is displayed on the final row. The data comprises of monthly nominal zero coupon bonds from October 1986 to August 2014.

Table 2: Evaluation of alternative specifications of the three factor standard AFNS model for nominal rates.

Alternative specifications	logL	k	p-value	AIC	BIC
(1) Unrestricted $\kappa^{\mathbb{P}}$	13324.1389	23		-26602.2779	-26514.5529
(2) $\kappa^{\mathbb{P}}_{31} = 0$	13324.1386	22	0.9803	-26604.2773	-26520.3664
(3) $\kappa^{\mathbb{P}}_{31} = \kappa^{\mathbb{P}}_{32} = 0$	13324.1379	21	0.9993	-26606.2759	-26526.1791
(4) $\kappa^{\mathbb{P}}_{31} = \kappa^{\mathbb{P}}_{32} = \kappa^{\mathbb{P}}_{21} = 0$	13324.1174	20	0.9978	-26608.2347	-26531.9521
(5) $\kappa^{\mathbb{P}}_{31} = ... = \kappa^{\mathbb{P}}_{12} = 0$	13324.0991	19	0.9998	-26610.1982	-26537.7297
(6) $\kappa^{\mathbb{P}}_{31} = ... = \kappa^{\mathbb{P}}_{13} = 0$	13323.8107	18	0.9890	**-26611.6215**	-26542.9671
(7) $\kappa^{\mathbb{P}}_{31} = ... = \kappa^{\mathbb{P}}_{23} = 0$	13321.4142	17	0.5706	-26608.8284	**-26543.9882**

NOTE: We estimate and evaluate seven alternative specifications of the individual standard AFNS model on nominal yields. For each specification, we record its log-likelihood (LogL), number of parameters (k) and the p-value of a likelihood ratio test of the hypothesis that a specification with (k-i) parameters is different from the one with (k-i+1) parameters. The information criteria (AIC and BIC) are reported and we display their minimum in bold.

Table 3: Three factor standard AFNS estimates for nominal rates.

$\kappa_t^{\mathbb{P}}$	$\kappa_{.,1}^{\mathbb{P}}$	$\kappa_{.,2}^{\mathbb{P}}$	$\kappa_{.,3}^{\mathbb{P}}$	θ^P	$\sigma_{i,i}^N$
$\kappa_{1,.}^{\mathbb{P}}$	0.0848	0.0000	0.0000	0.0824	0.0118
	(0.031624)			(0.031623)	(0.033686)
$\kappa_{2,.}^{\mathbb{P}}$	0.0000	0.3706	-0.2413	-0.0214	0.0174
		(0.031623)	(0.031623)	(0.031631)	(0.033907)
$\kappa_{3,.}^{\mathbb{P}}$	0.0000	0.0000	0.4538	-0.0103	0.0304
			(0.031623)	(0.031628)	(0.031768)

NOTE: The estimated parameters of the $\kappa^{N,\mathbb{P}}$ matrix, $\theta^{N,\mathbb{P}}$ vector, and diagonal diffusion matrix $\sigma_{i,i}^N$ are given for our preferred individual three-factor standard AFNS model for nominal yields. The estimated value of λ^N is 0.4321 with standard deviation of 0.031623. The numbers in parentheses are the standard deviations of the estimated parameters.

Table 4: Measures of fit for the three factor standard AFNS model for nominal yields.

Maturity in months	Mean(in bp)	RMSE(in bp)
6	-0.0315	6.3691
12	0.0000	0.0000
24	-0.1829	1.7789
36	0.0000	0.0000
60	0.1765	2.2207
84	-0.0231	1.3562
120	-0.7272	11.9314

NOTE: The mean and RMSE of fitted errors of the preferred individual three-factor standard AFNS model for nominal yields are given. All values are measured in basis points. The nominal yields span from October 1986 to August 2014.

Table 5: Evaluation of alternative specifications of the three factor shadow-rate AFNS model for nominal rates.

Alternative specifications	logL	k	p-value	AIC	BIC
(1) Unrestricted $\kappa^{\mathbb{P}}$	13591.3729	23		-27136.7458	-27049.0208
(2) $\kappa^{\mathbb{P}}_{31} = 0$	13591.3717	22	0.9614	-27138.7434	-27054.8326
(3) $\kappa^{\mathbb{P}}_{31} = \kappa^{\mathbb{P}}_{12} = 0$	13591.2280	21	0.8661	-27140.4559	-27060.3592
(4) $\kappa^{\mathbb{P}}_{31} = \kappa^{\mathbb{P}}_{12} = \kappa^{\mathbb{P}}_{32} = 0$	13591.1876	20	0.9940	-27142.3752	-27066.0926
(5) $\kappa^{\mathbb{P}}_{31} = ... = \kappa^{\mathbb{P}}_{13} = 0$	13590.6782	19	0.9069	**-27143.3564**	-27070.8879
(6) $\kappa^{\mathbb{P}}_{31} = ... = \kappa^{\mathbb{P}}_{21} = 0$	13589.1025	18	0.6767	-27142.2050	**-27073.5507**
(7) $\kappa^{\mathbb{P}}_{31} = ... = \kappa^{\mathbb{P}}_{23} = 0$	13586.1000	17	0.4226	-27138.1999	-27073.3597

NOTE: We estimate and evaluate seven alternative specifications of the individual shadow-rate AFNS model on nominal yields. For each specification, we record its log-likelihood (LogL), number of parameters (k) and the p-value of a likelihood ratio test of the hypothesis that a specification with (k-i) parameters is different from the one with (k-i+1) parameters. The information criteria (AIC and BIC) are reported and we display their minimum in bold.

Table 6: Three factor shadow-rate AFNS estimates for nominal rates.

$\kappa_t^{\mathbb{P}}$	$\kappa_{.,1}^{\mathbb{P}}$	$\kappa_{.,2}^{\mathbb{P}}$	$\kappa_{.,3}^{\mathbb{P}}$	θ^P	$\sigma_{i,i}^N$
$\kappa_{1,.}^{\mathbb{P}}$	0.0362	0.0000	0.0000	0.0513	0.0157
	(0.034041)			(0.007385)	(0.000488)
$\kappa_{2,.}^{\mathbb{P}}$	0.1103	0.3359	-0.2286	-0.0005	0.0206
	(0.072374)	(0.047283)	(0.032776)	(0.012462)	(0.000833)
$\kappa_{3,.}^{\mathbb{P}}$	0.0000	0.0000	0.4507	-0.0164	0.0324
			(0.031654)	(0.006607)	(0.001453)

NOTE: The estimated parameters of the $\kappa^{N,\mathbb{P}}$ matrix, $\theta^{N,\mathbb{P}}$ vector, and diagonal diffusion matrix $\sigma_{i,i}^N$ are given for our preferred individual three-factor shadow-rate AFNS model for nominal yields. The estimated value of λ^N is 0.4622 with standard deviation of 0.009396. The numbers in parentheses are the standard deviations of the estimated parameters.

Table 7: Measures of fit for the three factor shadow-rate AFNS model for nominal yields.

Maturity in months	Mean(in bp)	RMSE(in bp)
6	-0.5525	6.2018
12	0.2633	1.1375
24	0.2965	2.0152
36	0.3646	1.8497
60	0.5441	3.7132
84	0.4890	3.6883
120	-0.3768	10.0980

NOTE: The mean and RMSE of fitted errors of the preferred individual three-factor shadow-rate AFNS model for nominal yields are given. All values are measured in basis points. The nominal yields span from October 1986 to August 2014.

Table 8: First three principal components in real yields.

Maturity	First PC	Second PC	Third PC
60 months	0.4321	0.6563	0.5152
72 months	0.4199	0.3210	-0.2525
84 months	0.4099	0.0396	-0.4941
96 months	0.4017	-0.1922	-0.3526
108 months	0.3949	-0.3805	0.0350
120 months	0.3893	-0.5320	0.5488
% explained	98.96	1.03	0.01

NOTE: We provide the loadings of the yields of the set of maturities on the first three principal components. The percentage of all real bond yields' cross-sectional variation accounted for by each component is displayed on the final row. The data comprises of monthly real zero coupon bonds from October 1986 to August 2014.

Table 9: Evaluation of alternative specifications of the three factor standard AFNS model for real rates.

Alternative specifications	logL	k	p-value	AIC	BIC
(1) Unrestricted $\kappa^{\mathbb{P}}$	14751.0538	22		-29456.1075	-29374.1966
(2) $\kappa^{\mathbb{P}}_{21} = 0$	14751.0537	21	0.9902	-29458.1074	-29380.0106
(3) $\kappa^{\mathbb{P}}_{21} = \kappa^{\mathbb{P}}_{12} = 0$	14750.7779	20	0.7590	-29459.5559	-29385.2732
(4) $\kappa^{\mathbb{P}}_{21} = \kappa^{\mathbb{P}}_{12} = \kappa^{\mathbb{P}}_{31} = 0$	14750.7777	19	1.0000	-29463.5553	-29391.0869
(5) $\kappa^{\mathbb{P}}_{21} = ... = \kappa^{\mathbb{P}}_{32} = 0$	14750.7593	18	0.9998	-29463.5186	-29396.8643
(6) $\kappa^{\mathbb{P}}_{21} = ... = \kappa^{\mathbb{P}}_{23} = 0$	14750.7287	17	1.0000	**-29465.4574**	**-29402.6172**
(7) $\kappa^{\mathbb{P}}_{21} = ... = \kappa^{\mathbb{P}}_{13} = 0$	14747.7547	16	0.4290	-29461.5093	-29402.4832

NOTE: We estimate and evaluate seven alternative specifications of the individual standard AFNS model on real yields. For each specification, we record its log-likelihood (LogL), number of parameters (k) and the p-value of a likelihood ratio test of the hypothesis that a specification with k-i parameters is different from the one with k-i+1 parameters. The information criteria (AIC and BIC) are reported and we display their minimum in bold.

Table 10: Three factor standard AFNS estimates for real rates.

$\kappa_t^{\mathbb{P}}$	$\kappa_{.,1}^{\mathbb{P}}$	$\kappa_{.,2}^{\mathbb{P}}$	$\kappa_{.,3}^{\mathbb{P}}$	θ^P	$\sigma_{i,i}^R$
$\kappa_{1,.}^{\mathbb{P}}$	0.0856	0.0000	0.0109	0.0122	0.0047
	(0.031623)		(0.031623)	(0.031623)	(0.031623)
$\kappa_{2,.}^{\mathbb{P}}$	0.0000	0.1000	0.0000	0.0006	0.0428
		(0.031623)		(0.031623)	(0.031623)
$\kappa_{3,.}^{\mathbb{P}}$	0.0000	0.0000	0.0984	-0.0058	0.0460
			(0.031623)	(0.031623)	(0.031623)

NOTE: The estimated parameters of the $\kappa^{R,\mathbb{P}}$ matrix, $\theta^{R,\mathbb{P}}$ vector, and diagonal diffusion matrix $\sigma_{i,i}^R$ are given for our preferred individual three-factor standard AFNS model for real yields. The estimated value of λ^R is 0.4521 with standard deviation of 0.031623. The numbers in parentheses are the standard deviations of the estimated parameters.

Table 11: Measures of fit for the three factor standard AFNS model for real yields.

Maturity in months	Mean (in bp)	RMSE (in bp)
60	0.1729	1.0881
72	-0.0004	0.0028
84	0.0000	0.0006
96	0.0096	0.1299
108	0.0000	0.0002
120	0.0260	0.4806

NOTE: The mean and RMSE of fitted errors of the preferred individual three-factor standard AFNS model for real yields are given. All values are measured in basis points. The real yields span from October 1986 to August 2014.

Table 12: First six principal components in nominal and real yields.

Maturity	First PC	Second PC	Third PC	Fourth PC	Fifth PC	Sixth PC
NOMINAL YIELDS						
6 months	0.3847	-0.3487	-0.3801	0.4694	0.2793	-0.3865
12 months	0.3770	-0.2730	-0.2974	0.1014	-0.0291	0.2975
24 months	0.3643	-0.1659	-0.1430	-0.2685	-0.2530	0.4030
36 months	0.3530	-0.0934	0.0014	-0.4084	-0.2741	0.0602
60 months	0.3332	-0.0259	0.2525	-0.3253	-0.1044	-0.4754
84 months	0.3151	-0.0143	0.4397	-0.0662	0.1222	-0.3622
120 months	0.2889	-0.0119	0.6081	0.2857	0.3787	0.4846
REAL YIELDS						
60 months	0.1679	0.4209	-0.2703	-0.3109	0.5017	0.0527
72 months	0.1649	0.3930	-0.1787	-0.1014	0.2335	0.0142
84 months	0.1627	0.3656	-0.1026	0.0621	0.0102	-0.0079
96 months	0.1612	0.3396	-0.0404	0.1856	-0.1708	-0.0186
108 months	0.1601	0.3155	0.0099	0.2764	-0.3135	-0.0208
120 months	0.1593	0.2939	0.0505	0.3421	-0.4230	-0.0163
% explained	95.41	2.86	1.59	0.11	0.03	0.01

NOTE: We provide the loadings of the yields of the set of maturities on the first three principal components. The percentage of all nominal and real bond yields' cross-sectional variation accounted for by each component is displayed on the final row. The data comprises of monthly nominal and real zero coupon bonds from October 1986 to August 2014.

Table 13: Evalutation of alternative specifications of the five factor joint shadow-rate AFNS model.

Alternative specifications	logL	k	p-value	AIC	BIC
(1) Unrestricted $\kappa^{\mathbb{P}}$	26479.9718	51		-52857.9436	-52663.4229
(2) $\kappa^{\mathbb{P}}_{32} = 0$	26479.9718	50	0.9997	-52859.9436	-52669.2371
(3) $\kappa^{\mathbb{P}}_{32} = \kappa^{\mathbb{P}}_{53} = 0$	26479.9401	49	0.9688	-52861.8803	-52674.9879
(4) $\kappa^{\mathbb{P}}_{32} = \kappa^{\mathbb{P}}_{53} = \kappa^{\mathbb{P}}_{41} = 0$	26479.9385	48	1.0000	-52863.8771	-52680.7988
(5) $\kappa^{\mathbb{P}}_{32} = ... = \kappa^{\mathbb{P}}_{21} = 0$	26479.9302	47	1.0000	-52865.8603	-52686.5962
(6) $\kappa^{\mathbb{P}}_{32} = ... = \kappa^{\mathbb{P}}_{12} = 0$	26479.8202	46	0.9989	-52867.6404	-52692.1904
(7) $\kappa^{\mathbb{P}}_{32} = ... = \kappa^{\mathbb{P}}_{45} = 0$	26479.4495	45	0.9936	-52868.8990	-52697.2631
(8) $\kappa^{\mathbb{P}}_{32} = ... = \kappa^{\mathbb{P}}_{23} = 0$	26479.3606	44	1.0000	-52870.7212	-52702.8995
(9) $\kappa^{\mathbb{P}}_{32} = ... = \kappa^{\mathbb{P}}_{31} = 0$	26479.2732	43	1.0000	-52872.5463	-52708.5387
(10) $\kappa^{\mathbb{P}}_{32} = ... = \kappa^{\mathbb{P}}_{42} = 0$	26479.2140	42	1.0000	-52874.4281	-52714.2346
(11) $\kappa^{\mathbb{P}}_{32} = ... = \kappa^{\mathbb{P}}_{13} = 0$	26479.1388	41	1.0000	-52876.2777	-52719.8983
(12) $\kappa^{\mathbb{P}}_{32} = ... = \kappa^{\mathbb{P}}_{15} = 0$	26479.0554	40	1.0000	-52878.1108	-52725.5455
(13) $\kappa^{\mathbb{P}}_{32} = ... = \kappa^{\mathbb{P}}_{54} = 0$	26479.0141	39	1.0000	-52880.0282	-52731.2771
(14) $\kappa^{\mathbb{P}}_{32} = ... = \kappa^{\mathbb{P}}_{43} = 0$	26477.7390	38	0.9991	-52879.4779	-52734.5410
(15) $\kappa^{\mathbb{P}}_{32} = ... = \kappa^{\mathbb{P}}_{24} = 0$	26477.4785	37	1.0000	-52880.9571	-52739.8343
(16) $\kappa^{\mathbb{P}}_{32} = ... = \kappa^{\mathbb{P}}_{51} = 0$	26477.4201	36	1.0000	-52882.8403	-52745.5316
(17) $\kappa^{\mathbb{P}}_{32} = ... = \kappa^{\mathbb{P}}_{52} = 0$	26477.1339	35	1.0000	-52884.2677	-52750.7732
(18) $\kappa^{\mathbb{P}}_{32} = ... = \kappa^{\mathbb{P}}_{14} = 0$	26475.9635	34	1.0000	-52883.9270	-52754.2466
(19) $\kappa^{\mathbb{P}}_{32} = ... = \kappa^{\mathbb{P}}_{25} = 0$	26475.0090	33	1.0000	-52884.0179	-52758.1516
(20) $\kappa^{\mathbb{P}}_{32} = ... = \kappa^{\mathbb{P}}_{34} = 0$	26475.7065	32	1.0000	-52887.4131	-52765.3609
(21) $\kappa^{\mathbb{P}}_{32} = ... = \kappa^{\mathbb{P}}_{35} = 0$	26475.2570	31	1.0000	**-52888.5140**	**-52770.2759**

NOTE: We estimate and evaluate thirteen alternative specifications of the joint shadow-rate AFNS model on nominal and real yields. For each specification, we record its log-likelihood (LogL), number of parameters (k) and the p-value of a likelihood ratio test of the hypothesis that a specification with (k-i) parameters is different from the one with (k-i+1) parameters. The information criteria (AIC and BIC) are reported and we display their minimum in bold.

Table 14: Five factor joint shadow-rate AFNS estimates.

$\kappa_t^{\mathbb{P}}$	$\kappa_{.,1}^{\mathbb{P}}$	$\kappa_{.,2}^{\mathbb{P}}$	$\kappa_{.,3}^{\mathbb{P}}$	$\kappa_{.,4}^{\mathbb{P}}$	$\kappa_{.,5}^{\mathbb{P}}$	θ^P	$\sigma_{i,i}^J$
$\kappa_{1,.}^{\mathbb{P}}$	0.0311	0.0000	0.0000	0.0000	0.0000	0.0738	0.0127
	(0.031623)					(0.031624)	(0.031891)
$\kappa_{2,.}^{\mathbb{P}}$	0.0000	0.0458	0.0000	0.0000	0.0000	0.0107	0.0191
		(0.031623)				(0.031626)	(0.031624)
$\kappa_{3,.}^{\mathbb{P}}$	0.0000	0.0000	0.1163	0.0000	0.0000	-0.0919	0.0291
			(0.031623)			(0.031628)	(0.031627)
$\kappa_{4,.}^{\mathbb{P}}$	0.0000	0.0000	0.0000	0.1381	0.0000	-0.0006	0.0204
				(0.031623)		(0.031627)	(0.031836)
$\kappa_{5,.}^{\mathbb{P}}$	0.0000	0.0000	0.0000	0.0000	0.0958	-0.0128	0.0225
					(0.031623)	(0.031623)	(0.031829)

NOTE: The estimated parameters of the $\kappa^{J,\mathbb{P}}$ matrix, $\theta^{J,\mathbb{P}}$ vector, and diagonal diffusion matrix $\sigma_{i,i}^J$ are given for our preferred joint five-factor shadow-rate AFNS model for nominal and real yields. The estimated value of λ^N is 0.5005 with standard deviation of 0.031623 and the estimated value of λ^R is 0.2209 with standard deviation of 0.031635. The estimated value of α^R is 0.5781 with standard deviation of 0.031623. The numbers in parentheses are the standard deviations of the estimated parameters.

Table 15: Measures of fit for the five factor joint shadow-rate AFNS model.

Maturity in months	Mean(in bp)	RMSE(in bp)
Nominal yield		
6	-0.6420	6.0045
12	0.2150	0.9538
24	0.2800	1.8470
36	0.2938	1.3302
60	0.3302	2.6903
84	0.4321	2.3452
120	0.9552	10.3274
Real yield		
60	-0.5442	6.3068
72	-0.1748	1.8816
84	0.0000	0.0000
96	0.0000	0.0000
108	-0.1288	1.2824
120	-0.3094	3.3365

NOTE: The mean and RMSE of fitted errors of the preferred joint shadow-rate AFNS model for nominal and real yields are given. All values are measured in basis points. The nominal and real yields span from October 1986 to August 2014.
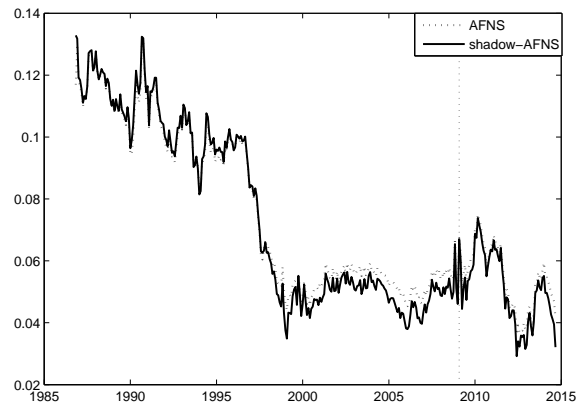
(a) Level factor
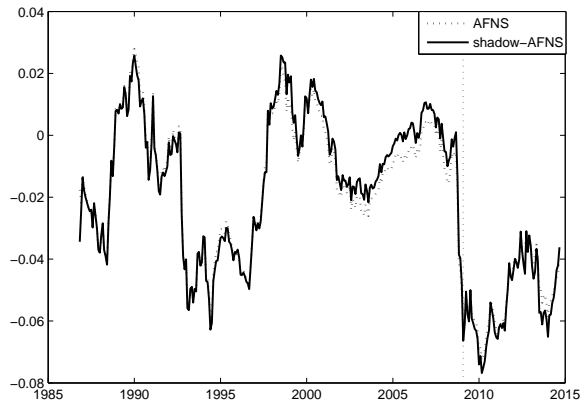
(b) Slope factor
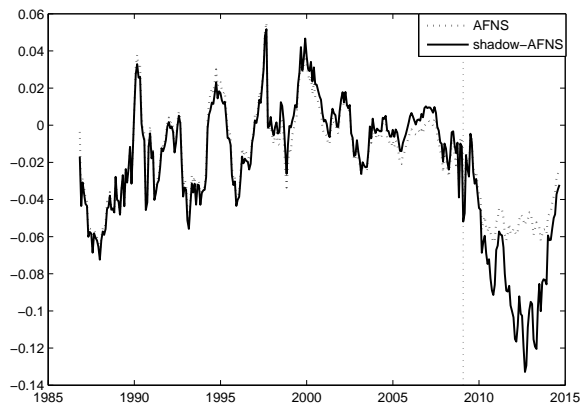
(c) Curvature factor

Figure 1: **Estimated State Variables.**

State variables, estimated with the AFNS and shadow-rate AFNS models.

44
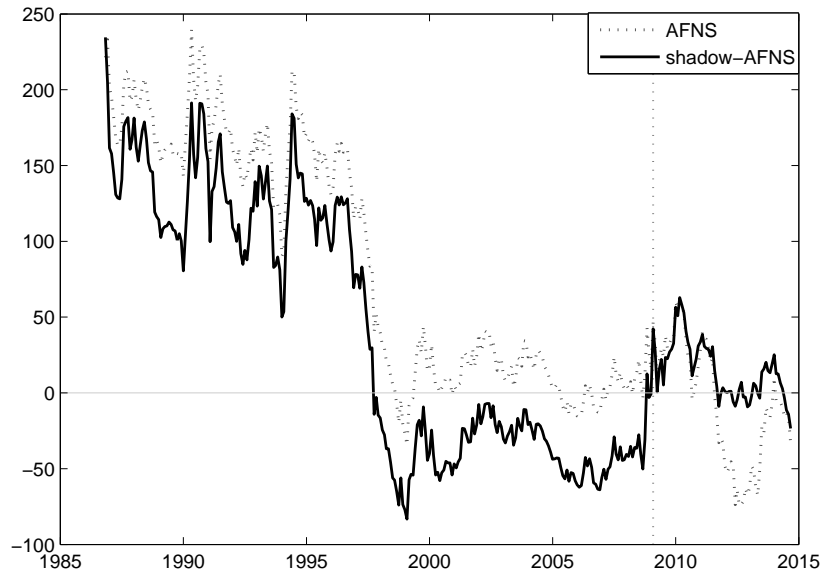
(a) Fitted Ten-Year Term Premium
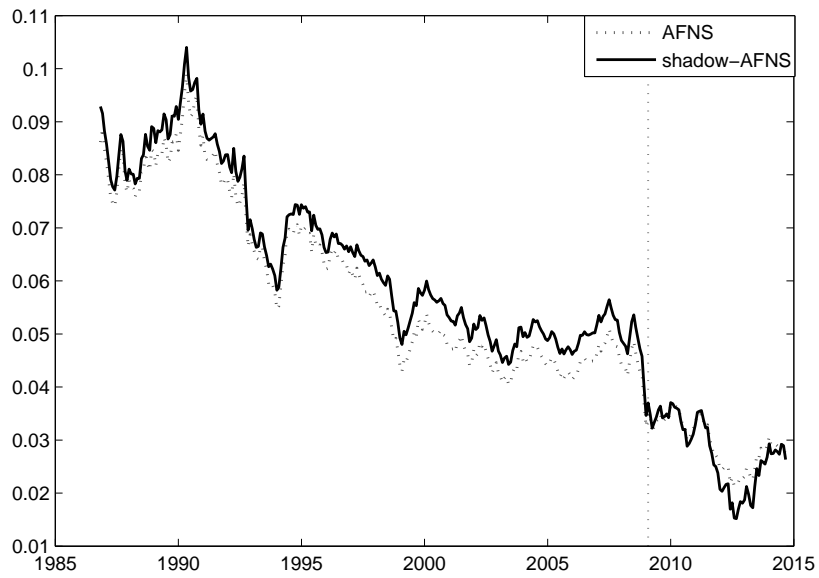
(b) Fitted expectation term of the ten-year yield

Figure 2: **Fitted Ten-Year Term Premium and Expectation Component.**
Ten-year fitted term premia of nominal yields and fitted expectation term of the ten-year yield, measured in basis points, estimated with the preferred AFNS and shadow-rate AFNS models.
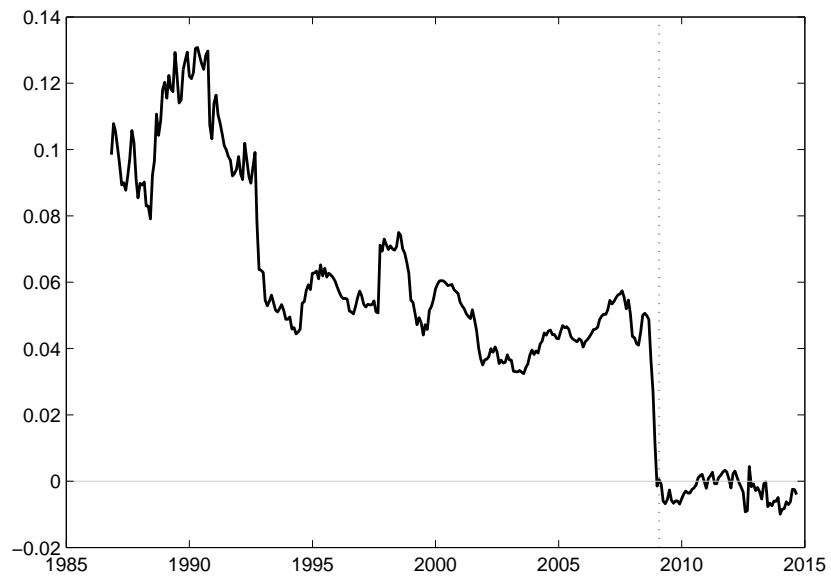
Figure 3: **Estimated Shadow Rate.**

Shadow rate process, estimated with the preferred shadow-rate AFNS models.
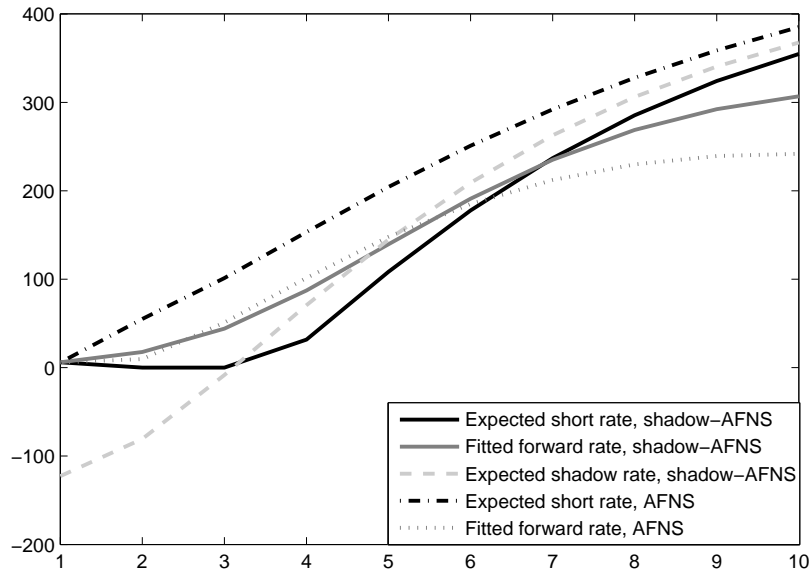
(a) June 2012
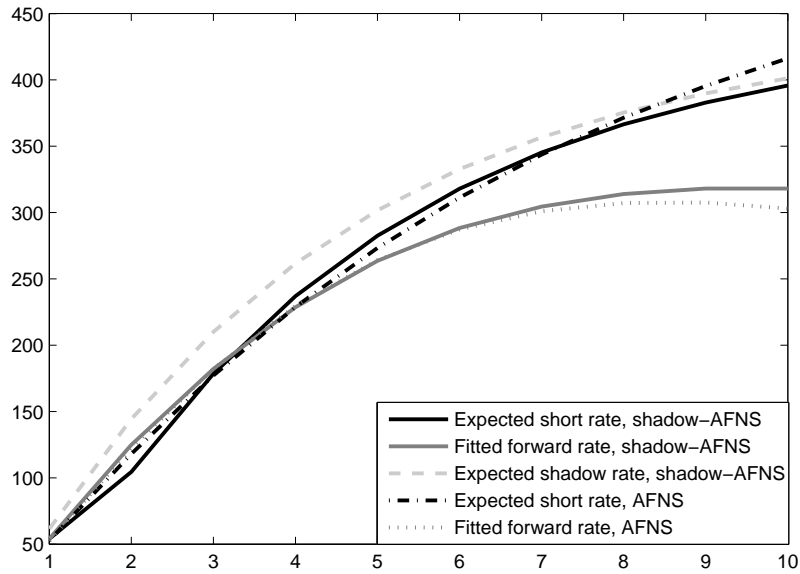
(b) August 2014

Figure 4: **Forward Rates and Expected Short Rates.**

Estimated forward rates and the associated short rate path implied by the AFNS and shadow-rate AFNS models. All curves in subfigures (a) and (b) are extracted as of June 2012 and August 2014, respectively, and are measured in basis points.

(a) Inflation Expectations, RPI Inflation and RPI Inflation Target Level by Maturity
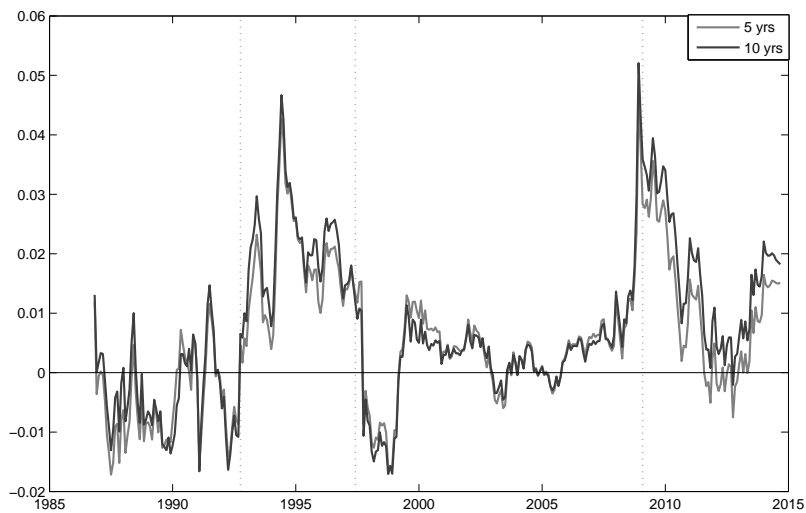
(b) Inflation Premia by Maturity

Figure 5: **Five- and Ten-Year Breakeven Rate Decomposed in Inflation Expectation and Inflation Risk Premium.**

The 5- and 10- year expected inflation rates and inflation risk premia, implied from the preferred joint shadow-rate AFNS model, historical RPI inflation and RPI inflation target. The data span from October 1986 to August 2014.
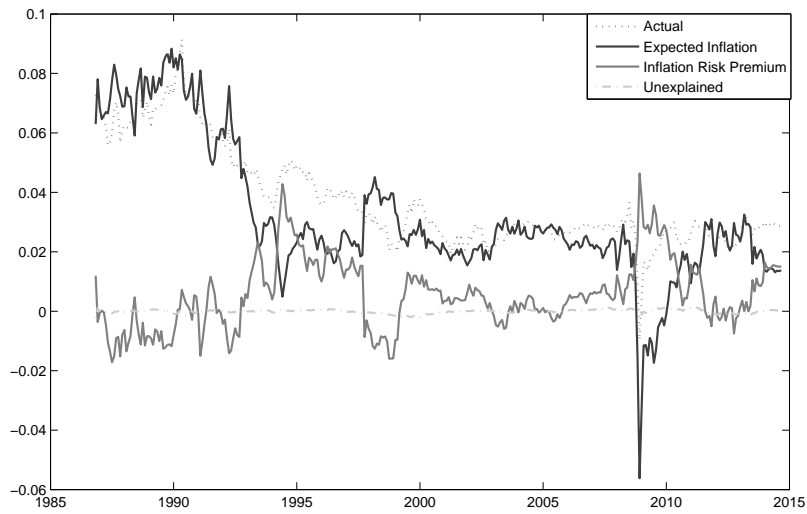
(a) 5-year maturity
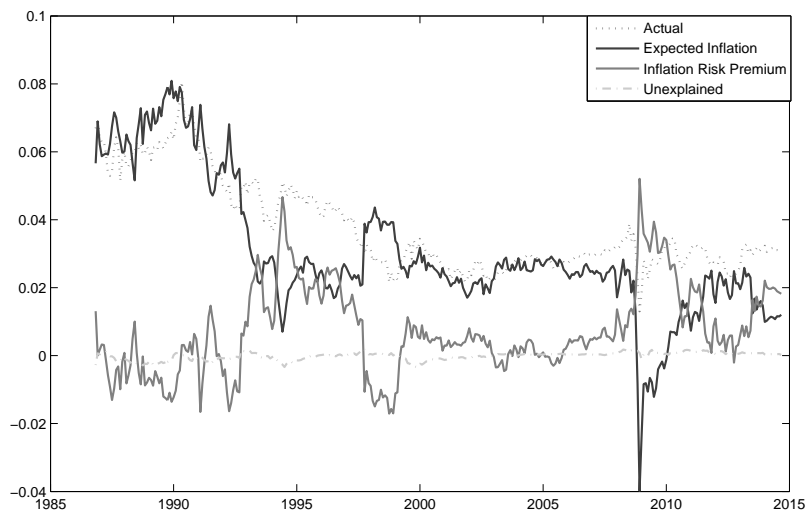
(b) 10-year maturity

Figure 6: **Actual BEI Rates and Model-Implied Decompositions.**

The 5- and 10- year actual BEI rates and inflation expectation and risk premia components implied from the preferred joint AFNS model. The data span from October 1986 to August 2014.

Documents de Travail

570. G. Verdugo, "Real Wage Cyclicality in the Eurozone before and during the Great Recession: Evidence from micro data" September 2015

571. M. Bussière, L. Ferrara and J. Milovich, "Explaining the Recent Slump in Investment: the Role of Expected Demand and Uncertainty" September 2015

572. M. Albert, C. Jude and C. Rebillard, "The Long Landing Scenario: Rebalancing from Overinvestment and Excessive Credit Growth. Implications for Potential Growth in China" October 2015

573. P. Andrade, G. Gaballo, E. Mengus and B. Mojon, "Forward Guidance and Heterogeneous Beliefs" October 2015

574. C. Jadeau, E. Jousselin, S. Roux and G. Verdugo, "The behaviour of French Firms during the Crisis: Evidence from the Wage Dynamics Network Survey" October 2015

575. C. Berson and N. Ferrari, "Financial incentives and labor market duality" October 2015

576. K. Istrefi and B. Vonnak, "Delayed Overshooting Puzzle in Structural Vector Autoregression Models" October 2015

577. S. Avouyi-Dovi and J-G. Sahuc, "On the sources of macroeconomic stability in the euro area" November 2015

578. F. Canova, F. Ferroni and C. Matthes, "Approximating time varying structural models with time invariant structures" December 2015

579. R. Cezar and O. R. Escobar, "Institutional distance and foreign direct investment" December 2015

580. J. Carluccio, A. Cuñat, H. Fadinger and C. Fons-Rosen, "Offshoring and Skill-upgrading in French Manufacturing: A Heckscher-Ohlin-Melitz View" December 2015

581. G. Cette, R. Lecat et A. Ould Ahmed Jiddou, "Margin rate and the cycle: the role of trade openness" February 2016

582. G. Horny, S. Manganelli and B. Mojon, "Measuring Financial Fragmentation in the Euro Area Corporate Bond Market" February 2016

583. S. Osotimehin and F. Pappadà, "Credit frictions and the cleansing effect of recessions" March 2016

584. F. Langot and A. Pizzo, "Accounting for Labor Gaps" March 2016

585. P. Fève and J.-G. Sahuc, "In Search of the Transmission Mechanism of Fiscal Policy in the Euro Area" March 2016

586. G. Cette, J. Fernald and B. Mojon, "The Pre-Great Recession Slowdown in Productivity" March 2016

587. E. Gautier, D. Fougère and S. Roux, "The Impact of the National Minimum Wage on Industry-Level Wage Bargaining in France" March 2016

588. A. Bergeaud, G. Cette and R. Lecat, "The role of production factor quality and technology diffusion in 20th century productivity growth" April 2016

589. A. Carriero, S. Mouabbi and E. Vangelista, "UK term structure decompositions at the zero lower bound" April 2016